28(1-2)

28(1-2

# 気象庁欧文海洋報告

第28巻 第1-2号

LIBRARY

# THE OCEANOGRAPHICAL MAGAZINE

SEP 2 7 1977

Vol. 28 No. 1-2

## CONTENTS

ISOZAKI, I. and E. KITAHARA: Tides in the Bays of Ariake and Yatsushiro... 1
AKAGAWA, M.: Characteristics of Oceanographic Conditions in the Okhotsk Sea and Meteorological Conditions over the Far East in November ..... 33
KIMURA, T.: Visual Wave Observations on Board the R/V Keifu-maru..... 47

*Published by the Japan Meteorological Agency*

March, 1977

## 投稿規定

1　資　格

原則として，気象庁職員に限る。ただし，気象庁職員との連名の場合は，この限りでない。

2　論文及び報文（以下「論文等」という。）の内容

未発表の原稿で，海洋（物理・化学・生物・地質など）及び海上気象（波浪・海水・海気相互関係など）に関する論文並びに気象庁における海洋・海上気象業務の活動，そのために開発された測器及び方法に関する報文など。

3　書き方

(1) 用語は，欧文（原則として英文）とする。

(2) 論文等には，英文（300語以内）及び和文（800字以内）の要約を受ける。要約は，方法・測器・実験・観測の結果・仮定・理論などの中味が読みとれるように留意し，なるべく指定の長さで簡潔に書く。

(3) 論文等の始めには，題名・著者名及所属機関名を明記する。和文の要約にも同様のことを明記する。

(4) 原稿は，厚手の用紙にダブルスペースでタイプする。

(5) 図は，白紙又は青方眼紙に墨入れし，図及び図中の文字の大きさは，印刷の際の縮小率を考えて作成する。特に重要な図は，投稿者が大きさを指定する（印刷の都合上，希望どおりにならないこともある。）

(6) 図（写真を含む。）及び表には，必ず説明を付ける。図の説明文は，別紙にタイプする。折り込みの図及び表は，なるべく避ける。図及び表のそう入箇所を本文の欄外に記入する。

(7) 数式は，2行取りに書き，数式の文字及び記号をはっきりと説明する。

(8) 論文等の中に文献を引用する場合は，「Allen (1927)」又は「(Allen, 1927)」のように書く。

(9) 引用文献は，最後にまとめて付け，著者名のアルファベット順に並べる。書き方は次のようにする。

Allen, W.E. (1927): Surface catches of marine diatoms and dinoflagellates made by U.S.A. Pioneer in Alaskan waters in 1923. *Bull. Scripps Inst. Occanogr., Tech. Ser.* **1**(4), 39–48.

Budyko, M. I. (1956): *The heat balance of the earth's surface.* Hydrometeorogical Publishing House, Leningrad, pp. 254.

Veronins, G. and H. Stommel (1956): The action of a variable wind stress on a stratified ocean. *J. Mar. Res.*, **15**(1), 43–75.

4　提出方法

投稿票を付け，本稿のほかにコピー（図及び表を含む。）2部を添える。

5　締切り

毎年気象庁公報により公示する。

6　送付先

気象庁海洋気象部海洋課

（原則として，書留便で送付する。）

7　その他

論文1等編につき別刷り50部を著者に無料で送付する。

Oceanographical Magazine

編集委員長　Editor

安井　正，M. YASUI

編集委員　Editorial Board

半沢　正男，M. HANZAWA*
磯崎　一郎，I. ISOZAKI**
小長　俊二，S. KONAGA**
杉村　行勇，Y. SUGIMURA**
長坂　昂一，K. NAGASAKA*
飯田　隼人，H. IIDA*
川原田　裕，Y. KAWARADA***
窪田　将，M. KUBOTA***
鈴置　哲朗，T. SUZUOKI*

* 気象庁 JAPAN METEOROLOGICAL AGENCY

** 気象研究所 METEOROLOGICAL RESEARCH INSTITUTE

*** 気象大学校 METEOROLOGICAL COLLEGE

The Oceanographical Magazine
Vol. 28, Nos, 1-2, pp. 1 to 32, March 1977

# Tides in the Bays of Ariake and Yatsushiro

Ichiro Isozaki and Eiko Kitahara
*Meteorological Research Institute*

***Abstract***: In the present paper, we try to understand tidal phenomena in the Bays of Ariake and Yatsushiro systematically based on analysis of observed data and numerical experiment. Tide range, tidal current, tidal residual current and inclination of mean sea level in these bays are discussed. These are modified largely from the feature of astronomical tides by meteorological effects in addition to nonlinear processes due to large tide range and complicated topography.

## 1. Introduction

The Bay of Ariake is 90 km in length, 17 km in mean width, 1700 km$^2$ in area, 20 m in mean depth, and has hook-shaped configuration bent sharply at the central part as shown in Fig. 1. The bay connects with the East China Sea through the Hayasaki Straits. Vast tide land, constructed in its innermost part by earth and sand from many rivers such as Chikugo-gawa, Yabe-kawa, Shira-kawa, Midori-kawa, Rokkaku-gawa and Honmyo-gawa, has a width about 6~10 km outside the coast in ebb stage of spring tide.

The bay of Yatsushiro is 60 km in length, 1200 km$^2$ in area, 23 m in mean depth, and has complicated topography containing many small islands and straits. The bay connects with the East China Sea through the Nagashima Straits and Kuro-seto Straits, the latter of which has negligible effect on the exchange of water between inside and outside of the bay because of its narrow cross section. The bay has also vast tide land in its innermost part.

The Bay of Yatsushiro connects with the Bay of Ariake through two straits, Misumi-seto and Yanagi-seto. The word, "-seto", means narrow straits in Japanese. The Misumi-seto is 400 m in width and 30 m in mean depth, and the Yanagi-seto is 1100 m in width and 12 m in mean depth. These straits have no significant effect on the mutual exchange of water in both bays because of their narrow cross section.

The Bays of Ariake and Yatsushiro have the most predominant tidal oscillations in the coasts of the Japanese Islands. Tide range of them exceeds 500 cm and 320 cm

Fig. 1. Location of tide gage stations in the Bays of Ariake and Yatsushiro.

at respective bay head in a spring tide. Many investigations have been made on the large tide range in these bays because of their significant influence on construction of marine facilities, navigation, fishing, reclamation works, etc.

Ogura (1933) described rough natures of them in his vast investigation on the tide in the sea adjucent to Japan. Nagasaki Marine Observatory (1954, 1955) gave supplementary descriptions based on the analysis of many tidal observations. It was concluded in these investigations that semidiurnal tide develops conspicuously in the Bay of Ariake, and its range at the bay head becomes about 1.7 times as large as that at the mouth owing to a resonant mechanism of the proper oscillation of bay water with the astronomical tide outside the bay, contrary to diurnal tide whose range remains

nearly constant in the whole basin.

Nagasaki Marine Observatory (1959, 1961) performed model experiment on the tidal processes in the Bay of Ariake to help planning of reclamation works. Similarity of their model was satisfactory in spite of the small scale and extreme distortion in the scale of the model. They also examined effect of a dike proposed to reduce tidal amplitude in the bay.

Isozaki and Unoki (1964) applied a numerical model to the investigation of tide in the Bay of Ariake and examined the accuracy and the usefulness of the model. Their computation showed reasonable agreement with observation in the bay which is rather shallow. They emphasized that the nonlinear terms in the equation of motion are so dominant in the Bay of Ariake that reliable results will not be able to be expected without taking them into consideration.

Complexities of tidal phenomena in the Bay of Ariake and Yatsushiro are also due to large amount of fresh water inflow from many rivers, formation of spacious tide land, and meteorological effects. In spite of significant tidal influences on daily living and marine development we have only a few reliable tide records in these bays because the large tide range and the formation of spacious tide land prevent construction of tide gage station and continuation of reliable tide recording. So the characteristics of tide in these bays are still not well known in detail.

In the present paper, we intend to describe some features of tide in the Bays of Ariake and Yatsushiro based on analysis of tidal records and numerical experiment.

## 2. Numerical experiment

As has been outlined in the previous section, tidal phenomena in the Bays of Ariake and Yatsushiro are very complicated because of prevailing nonlinear processes caused by their large tide range and topographical influence. Additionally, accurate tidal observations are still not enough to discuss detailed tidal behavior in these bays. So we try to explain some characteristics of tide in these bays by the aid of numerical experiment. The numerical model used here is essentially the same as the one developed by Isozaki and Unoki (1964), accuracy and usefulness of which was recognized through the computation of tide in the Bays of Ariake and Tokyo.

### 2.1 Basic equations

In the usual equation of motion and that of continuity, we assume that the pressure is hydrostatic. Integrating these equations over depth from the surface $z=-\zeta(x, y, t)$ to the bottom $z=h(x, y)$ and neglecting the terms of higher order, we have

$$\frac{\partial M_x}{\partial t}=-g(h+\zeta)\frac{\partial \zeta}{\partial x}+\frac{\tau_s{}^{(x)}}{\rho_w}-\frac{\tau_b{}^{(x)}}{\rho_w}+fM_y-(h+\zeta)\left\{\frac{\partial \bar{u}^2}{\partial x}+\frac{\partial(\bar{u}\,\bar{v})}{\partial y}\right\} \tag{1}$$

$$\frac{\partial M_y}{\partial t}=-g(h+\zeta)\frac{\partial \zeta}{\partial y}+\frac{\tau_s{}^{(y)}}{\rho_w}-\frac{\tau_b{}^{(y)}}{\rho_w}-fM_x-(h+\zeta)\left\{\frac{\partial(\bar{u}\bar{v})}{\partial x}+\frac{\partial \bar{v}^2}{\partial y}\right\} \tag{2}$$

$$\frac{\partial \zeta}{\partial t}=-\frac{\partial M_x}{\partial x}-\frac{\partial M_y}{\partial y} \tag{3}$$

where $x$ and $y$ are the horizontal rectangular coordinates taken on the undisturbed sea surface, $z$ the vertical coordinate drawn downward, $f$ the Coriolis parameter, $\rho_w$ the density of sea water, $p$ the pressure, $g$ the acceleration of gravity, $\zeta$ the elevation of the sea surface, $h$ the depth of basin, $\bar{u}$ and $\bar{v}$ the components of the mean velocity $\bar{V}$, $\tau_s{}^{(x)}$ and $\tau_s{}^{(y)}$ the components of surface stress due to wind $\boldsymbol{\tau}_s$, $\tau_b{}^{(x)}$ and $\tau_b{}^{(y)}$ the components of bottom friction $\boldsymbol{\tau}_b$. $M_x$ and $M_y$ the components of the volume transport, being written as

$$M_x=(h+\zeta)\,\bar{u}=\int_{-h}^{\zeta} u\,dz \tag{4}$$

$$M_y=(h+\zeta)\,\bar{v}=\int_{-h}^{\zeta} v\,dz \tag{5}$$

As to the surface stress by wind and bottom friction our knowledge remains still uncertain and vague although a great deal of discussion have been made. Accordingly, for the present, they are given as follows

$$\boldsymbol{\tau}_s=\rho_a\gamma_a{}^2\boldsymbol{w}\,|\boldsymbol{w}| \tag{6}$$

$$\boldsymbol{\tau}_b=\rho^{\prime\prime}\gamma_w{}^2\boldsymbol{V}|\boldsymbol{V}|+\beta\boldsymbol{\tau}_s \tag{7}$$

where $\rho_a$ is the density of air, $\boldsymbol{w}$ the wind vector at an anemometer height and $\gamma_a{}^2$ the coefficient of surface stress. For $\gamma_a{}^2$ various values have been reported and reliable value has not been established yet. But it will be sure that the value depends on wind speed and we adopted the value $1.6\times10^{-3}$ expediently as a value corresponding to a wind speed 7 m/s. $\gamma_w{}^2$ is the coefficient of bottom friction and we used for it the same value as $\gamma_a{}^2$. $\beta$ is a constant and determined as 0.35 empirically.

Along a coastal boundary, water mass is assumed not to be transported across the coast line but can flow along the coast, that is,

$$M_n=0 \qquad \text{along the coast} \tag{8}$$

where the subscript $n$ means the normal to the coast.

Moreover, to complete the calculation, either the surface elevation or flow at the open end of the bay must be given. We usd the former, which can be given from observed values or periodic values assumed in such a way that

$$(\zeta)_{\text{mouth}} = \sum_i (H_0)_i \sin(\sigma_i t - \kappa_i) \tag{9}$$

where $(H_o)_i$, $\sigma_i$, and $k_i$ are the amplitude, the angular velocity and the phase constant of a component wave respectively.

### 2.2 Conditions of experiment

In order to solve the equations (1), (2) and (3) numerically they have to be approximated by difference equations with a time difference $\Delta t$ and a space difference $\Delta s$. Then the flow and the elevation at respective grid points were estimated step by step,

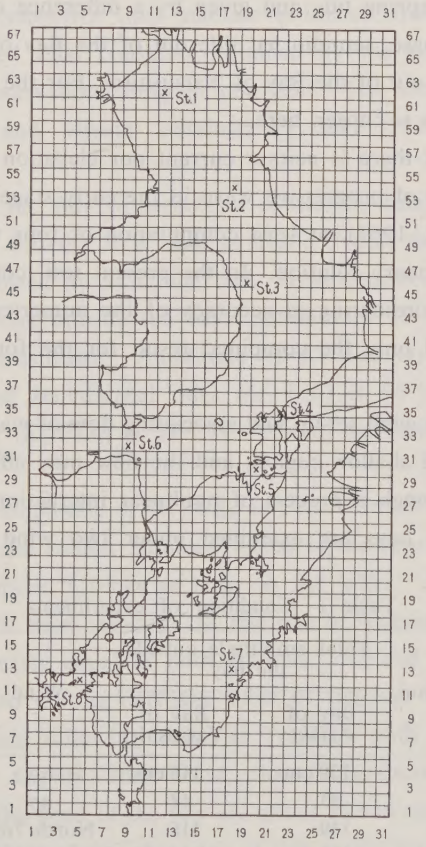


Fig. 2. Computation domain.

using the difference equations of motion and continuity alternatively. As the value of $\Delta s$ and $\Delta t$, in the present computation, 2 km and 45 seconds are chosen respectively, so as to fulfil the condition of computational stability. Computation area and grid used here are shown in Fig. 2.

The position of boundary facing open ocean directly, where tidal variation is given as a boundary condition, are chosen on south-to-north cross section through the station Tomioka for the Bay of Ariake and southeast-to-northwest cross section through the station Akune for the Bay of Yatsushiro. Tidal variation on these boundaries are given by use of Eq. (9), in which the constants are given by the tidal constants at Tomioka and Akune respectively.

In the present experiment, simulation of spring tide and neap tide is intended, so the value of amplitude in Eq. (9) is given by a sum of the amplitudes of $M_2$ and $S_2$ constituents in case of spring tide and given by a difference of them in case of neap tide. As to the tidal phase, semidiurnal tide out of the Bay of Ariake is assumed ten minutes behind the one out of the Bay of Yatsushiro. For the convenience of analysis, tidal period of 12 hours is chosen here.

Since we assume that there is neither current nor elevation in the bay initially, the calculated tide is a type of progressive wave in the early stage. According to previous test (Isozaki and Unoki, 1964), at least computation of four tidal cycles are required to get periodically stationary solution. In the present test, computation for four tidal cycles was performed considering in accuracy of the numerical model and economics of a computer use, and only the computed result for the fourth tidal cycle is taken and analysed.

There may be notable wind set-up and associating flow of water in these bays because of their widely spreaded shallow region, and the flow may affect significant influences on the tidal motion through a process of nonlinear interaction. So the characteristics of spring tide in these bays are examined under two wind conditions which have

Table 1 Condition of experiments

| | Tidal Condition | Tidal amplitude outside the bay | | Wind | Period and Phase |
|---|---|---|---|---|---|
| | | Bay of Ariake | Bay of Yatsushiro | | |
| Case–1 | Spring tide | 139 cm | 116 cm | no | $T=12^h$, $\kappa=0°$, Yatsushiro, $\kappa=10°$, Ariake |
| Case–2 | Neap tide | 53 | 48 | no | |
| Case–3 | Spring tide | 139 | 116 | North 7m/s | |
| Case–4 | Spring tide | 139 | 116 | South 7m/s | |

moderate speed of 7 m/s with directions of south and north respectively. These wind conditions seem to be representative of usual summer and winter wind situations. Conditions of four experiments made here are shown in Table 1.

### 3. Tidal amplitude

We have a few tidal stations in the Bays of Ariake and Yatsushiro for which accurate tidal constants have been determined in detail, because construction of the station and continuation of reliable tidal recording are prevented by the large tide range and formation of spacious tide land. In these circumstances, Nagasaki Marine Observatory (1954, 1955) obtained tidal constants shown in Table 2 based on the tidal harmonic analysis using tidal observations for a half of a month. Position of tidal stations in Table 2 is shown in Fig. 1. Table 3 shows mean tide range, spring tide range and neap tide range for respective tidal stations estimated from the value in Table 2. Table 4 shows detailed tidal constants obtained by the tidal harmonic analysis by use of recent tidal observations through one year. The table also contains the constants at Minamata and Misumi obtained by Seki (1948) and Miyazaki (1967) respectively.

Tidal oscillation in the Bay of Ariake is caused by tidal waves invading the bay through the Hayasaki Straits. It is seen in Table 2 that the most predominant tidal constituent is $M_2$ followed by $S_2$ in the bay. Now consider the tides at Tomioka as representative of the one outside the bay. Amplitudes of $M_2$ is about 2.2 times as large as that of $S_2$ constituent. Amplitude of $K_1$ and $O_1$ are about a half of $S_2$. Amplitude of principal semidiurnal tides $(M_2+S_2)$ is $96+43=139$ cm, the one of principal diurnal tides $(K_1+O_1)$ is $27+20=47$ cm, and the former is about 3 times as large as the latter.

On the other hand, amplitude of $(M_2+S_2)$ is $172+75=247$ cm and that of $(K_1+O_1)$ is $27+22=49$ cm at the station Suminoe which is the representative one on the bay head; the former is about 5 times as large as the latter. Amplitude of $(M_2+S_2)$ at Suminoe is about 1.78 times as large as the one at Tomioka, contrary to $(K_1+O_1)$ whose amplitude is nearly equal at both stations. $M_2$ and $S_2$ constituents at Kuchinotsu, which is situated on the northern coast of the bay mouth about 18 km apart from Tomioka, oscillate following those at Tomioka with delayed angle about 23° and 30° respectively. On the other hand, phase differences of both constituents between the mouth and the head of the bay are about 15° in spite of their distance 85 km along that bay axis. Most of the phase lag of tide inside the bay from the one outside

Table 2 Tidal constants (1)

| Station Name | | | $M_2$ | | $S_2$ | | $K_1$ | | $O_1$ | | $N_2$ | |
|---|---|---|---|---|---|---|---|---|---|---|---|---|
| | N | E | H cm | K ° | H cm | K ° | H cm | K ° | H cm | K ° | H cm | K ° |
| Tomioka | 32° 32′ | 130°02′ | 96 | 230 | 43 | 252 | 27 | 208 | 20 | 190 | | |
| | | | 88 | 219 | 41 | 255 | 25 | 208 | 20 | 183 | | |
| Kuchinotsu | 32° 36′ | 130°11′ | 104 | 254 | 41 | 290 | 28 | 216 | 21 | 192 | | |
| | | | 95 | 243 | 43 | 287 | 25 | 219 | 21 | 193 | | |
| Yanagi-seto | 32° 32′ | 130°25′ | 119 | 252 | 50 | 287 | 28 | 220 | 20 | 197 | | |
| | | | 114 | 252 | 49 | 281 | 27 | 219 | 18 | 187 | | |
| Misumi | 32° 37′ | 130°27′ | 125 | 254 | 52 | 295 | 26 | 220 | 19 | 201 | | |
| | | | 118 | 257 | 51 | 290 | 26 | 215 | 19 | 189 | | |
| Shimabara | 32° 47′ | 130°22′ | 147 | 258 | 56 | 299 | 25 | 219 | 20 | 204 | | |
| | | | 131 | 259 | 54 | 300 | 27 | 222 | 21 | 194 | | |
| Takesakijima | 32° 57′ | 130°13′ | 158 | 259 | 69 | 299 | 29 | 220 | 22 | 203 | | |
| | | | 158 | 259 | 71 | 296 | 28 | 221 | 21 | 197 | | |
| Miike | 33° 00′ | 130°23′ | 159 | 259 | 69 | 299 | 27 | 219 | 21 | 198 | | |
| | | | 155 | 267 | 69 | 302 | 30 | 222 | 21 | 203 | | |
| Wakatsu | 33° 13′ | 130°23′ | 161 | 262 | 68 | 301 | 25 | 228 | 20 | 193 | | |
| | | | 158 | 262 | 67 | 301 | 25 | 228 | 20 | 193 | | |
| Suminoe | 33° 12′ | 130°12′ | 172 | 267 | 75 | 306 | 27 | 221 | 22 | 206 | | |
| Oura | 32° 59′ | 130°13′ | 157.6 | 266.0 | 68.7 | 302.4 | 29.0 | 222.4 | 22.1 | 200.8 | 25.7 | 258.4 |
| Matsuai | 32° 37′ | 130°36′ | 110 | 259 | 53 | 288 | 23 | 223 | 20 | 197 | | |
| Kagashima | 32° 31′ | 130°32′ | 115 | 252 | 49 | 282 | 28 | 236 | 20 | 197 | | |
| Ikenoura | 32° 23′ | 130°21′ | 105 | 251 | 44 | 286 | 26 | 222 | 20 | 198 | | |
| Minamata | 32° 13′ | 130°23′ | 102.3 | 252.5 | 43.2 | 286.7 | 26.0 | 219.0 | 17.0 | 200.1 | 17.3 | 248.2 |
| Warabishima | 32° 07′ | 130°16′ | 102 | 252 | 49 | 276 | 25 | 223 | 20 | 191 | | |
| Ushibuka | 32° 12′ | 130°01′ | 85 | 226 | 36 | 255 | 26 | 209 | 20 | 189 | | |
| Sakitsuwan | 32° 19′ | 130°01′ | 83 | 224 | 39 | 251 | 24 | 205 | 20 | 189 | | |
| Akune | 32° 02′ | 130°11′ | 82 | 219 | 34 | 243 | 23 | 207 | 20 | 186 | | |

(from Nagasaki Marine Observatory, 1964)

Table 3 Tide range

| | Mean tide range (cm) | Spring tide range (cm) | Neap tide range (cm) |
|---|---|---|---|
| Tomioka | 192 | 278 | 106 |
| Kuchinotsu | 208 | 290 | 126 |
| Yanagi-seto | 238 | 338 | 138 |
| Misumi | 250 | 354 | 146 |
| Shimabara | 294 | 406 | 182 |
| Takesakijima | 316 | 454 | 178 |
| Miike | 318 | 456 | 180 |
| Wakatsu | 322 | 458 | 186 |
| Suminoe | 344 | 494 | 194 |
| Oura | 315 | 453 | 178 |
| Matsuai | 220 | 326 | 114 |
| Kagashima | 230 | 328 | 132 |
| Ikenoura | 210 | 298 | 122 |
| Minamata | 205 | 291 | 118 |
| Warabishima | 204 | 302 | 106 |
| Ushibuka | 170 | 242 | 98 |
| Sakitsuwan | 166 | 244 | 88 |
| Akune | 164 | 232 | 96 |

(from Nagasaki Marine Observatory, 1964)

the bay is concentrated near and around the bay mouth, and the tide inside the bay oscillates with almost same phase.

Notable development of the overtides and the compound tides which are usually produced by nonlinear processes in tidal oscillation represent the complexities of tide in the bay. Different kind of constituents in the overtides and the compound tides are predominant at respective stations, but amplitude of these constituents seems generally to become larger toward the northern end of the bay.

Tide in the Bay of Yatsushiro is caused by tidal waves invading the bay through the Nagashima Straits. Let consider the tide at Akune as representative of the one outside the bay. It is seen in Table 2 that the most predominant tidal constituent is $M_2$ followed by $S_2$. Amplitude of $M_2$ constituent is about 2.4 times as large as that of $S_2$ constituent. Amplitudes of $K_1$ and $O_1$ constituents are about 0.7 and 0.6 times as large as that of $S_2$ constituents respectively. Amplitude of principal semidiurnal tide ($M_2+S_2$) is $82+34=116$ cm, and that of principal diurnal tide ($K_1+O_1$) is $27+20=47$ cm; the former is about 2.7 times as large as the latter.

Table 4 Tidal

| | Oura | | Kuchinotsu | | Misumi | | Suminoe | | Miike | |
|---|---|---|---|---|---|---|---|---|---|---|
| | N 32° 59′ E 130° 13′ | | N 32° 36′ E 130° 12′ | | N 32° 37′ E 130° 27′ | | N 33° 12′ E 130° 13′ | | N 33° 01′ E 130° 35′ | |
| | H cm | *K* ° | H cm | *K* ° | H cm | *K* ° | H ° | *K* ° | H cm | *K* ° |
| Sa | 20.54 | 145.20 | 19.50 | 144.87 | 20.27 | 133.91 | 25.17 | 137.74 | 19.92 | 145.08 |
| Ssa | 6.52 | 263.42 | 5.33 | 265.02 | 1.96 | 270.67 | 4.84 | 274.31 | 5.50 | 264.71 |
| Mm | 1.26 | 314.36 | 1.60 | 244.49 | 1.68 | 81.69 | 2.82 | 39.67 | 1.43 | 325.21 |
| Msf | 1.26 | 349.33 | 2.62 | 231.99 | 1.40 | 15.33 | 3.03 | 18.39 | 1.20 | 353.56 |
| Mf | 1.25 | 170.70 | 1.67 | 184.39 | 0.77 | 200.48 | 2.40 | 134.43 | 1.33 | 167.96 |
| Mt | 0.92 | 107.01 | 0.70 | 103.97 | 0.78 | 62.15 | 1.97 | 79.21 | 0.84 | 107.19 |
| $2Q_1$ | 0.22 | 133.59 | 0.23 | 152.96 | 0.73 | 131.50 | 0.56 | 125.42 | 0.21 | 125.10 |
| $\sigma_1$ | 0.71 | 230.22 | 0.65 | 212.38 | 0.62 | 246.74 | 0.98 | 311.88 | 0.77 | 224.19 |
| $Q_1$ | 4.44 | 193.35 | 4.27 | 190.43 | 4.06 | 195.45 | 3.62 | 195.37 | 4.40 | 191.91 |
| $\delta_1$ | 0.64 | 177.94 | 0.69 | 188.40 | 0.58 | 228.33 | 0.63 | 130.35 | 0.72 | 184.43 |
| $O_1$ | 21.99 | 204.21 | 21.04 | 201.53 | 21.47 | 204.49 | 20.03 | 208.94 | 21.76 | 203.18 |
| $MP_1$ | 1.24 | 275.57 | 1.15 | 264.19 | 1.14 | 243.74 | 1.80 | 319.27 | 1.25 | 273.55 |
| $M_1$ | 1.45 | 159.56 | 1.28 | 155.32 | 1.33 | 115.74 | 1.52 | 184.64 | 1.44 | 158.21 |
| $\chi_1$ | 0.40 | 228.78 | 0.33 | 229.74 | 0.33 | 157.74 | 0.14 | 238.08 | 0.36 | 229.40 |
| $\pi_1$ | 0.29 | 267.44 | 0.33 | 248.07 | 0.43 | 251.17 | 0.69 | 294.67 | 0.29 | 249.23 |
| $P_1$ | 8.74 | 225.59 | 8.27 | 222.13 | 8.15 | 224.46 | 7.07 | 234.29 | 8.58 | 223.62 |
| $S_1$ | 0.18 | 59.67 | 0.08 | 100.99 | 0.49 | 110.94 | 1.15 | 169.54 | 0.34 | 88.25 |
| $K_1$ | 28.95 | 223.72 | 27.03 | 220.88 | 27.00 | 223.38 | 27.08 | 228.02 | 28.69 | 222.85 |
| $\psi_1$ | 0.24 | 301.31 | 0.25 | 285.34 | 0.36 | 217.86 | 0.53 | 286.03 | 0.34 | 299.82 |
| $\phi_1$ | 0.68 | 196.60 | 0.43 | 192.52 | 0.60 | 144.36 | .057 | 194.33 | 0.63 | 203.43 |
| $J_1$ | 1.80 | 252.99 | 1.70 | 245.98 | 1.90 | 253.60 | 1.16 | 266.31 | 1.73 | 250.27 |
| $SO_1$ | 1.22 | 352.17 | 1.02 | 336.11 | 1.01 | 344.32 | 2.63 | 25.19 | 1.24 | 354.23 |
| $OO_1$ | 0.97 | 296.53 | 0.84 | 288.47 | 0.83 | 300.72 | 1.05 | 315.14 | 0.99 | 295.49 |
| $\gamma_1$ | 0.24 | 316.75 | 0.23 | 297.71 | 0.40 | 268.02 | 0.33 | 39.01 | 0.26 | 305.37 |
| $OQ_2$ | 0.63 | 155.35 | 0.15 | 169.80 | 0.48 | 145.02 | 0.94 | 160.42 | 0.59 | 156.65 |
| $\varepsilon$ | 3.19 | 17.73 | 1.63 | 16.84 | 1.92 | 43.68 | 4.34 | 39.35 | 3.08 | 15.62 |
| $2N_2$ | 0.74 | 219.90 | 0.90 | 233.19 | 2.33 | 221.06 | 0.85 | 302.92 | 0.86 | 218.72 |
| $\mu_2$ | 11.25 | 321.21 | 6.39 | 314.62 | 8.47 | 313.21 | 14.44 | 343.97 | 11.07 | 320.83 |
| $N_2$ | 27.60 | 263.66 | 18.30 | 254.25 | 22.14 | 257.06 | 28.14 | 271.22 | 27.34 | 261.89 |

constants (2)

| | Oura | | Kuchinotsu | | Misumi | | Suminoe | | Miike | |
|---|---|---|---|---|---|---|---|---|---|---|
| | N 32° 59′ E 130° 13′ | | N 32° 36′ E 130° 12′ | | N 32° 37′ E 130° 27′ | | N 33° 12′ E 130° 13′ | | N 33° 01′ E 130° 25′ | |
| | H cm | K ° | H cm | K ° | H cm | K ° | H cm | K ° | H cm | K ° |
| $\nu_2$ | 5.39 | 247.50 | 3.87 | 253.06 | 4.40 | 242.77 | 4.53 | 242.76 | 5.25 | 250.34 |
| $OP_2$ | 1.89 | 237.24 | 0.60 | 189.24 | 0.93 | 181.11 | 1.25 | 237.93 | 2.04 | 211.50 |
| $\delta_2$ | 3.03 | 155.24 | 1.04 | 189.29 | 1.48 | 175.01 | 7.00 | 193.94 | 2.96 | 173.23 |
| $M_2$ | 155.16 | 268.59 | 102.52 | 260.51 | 120.87 | 262.49 | 160.69 | 276.73 | 152.68 | 267.22 |
| $\lambda_2$ | 4.46 | 241.47 | 2.98 | 232.93 | 3.98 | 228.56 | 5.56 | 255.36 | 4.28 | 237.49 |
| $L_2$ | 5.10 | 235.99 | 3.16 | 232.67 | 4.22 | 235.01 | 7.09 | 244.03 | 5.29 | 237.01 |
| $T_2$ | 4.65 | 312.49 | 2.14 | 290.62 | 3.44 | 314.20 | 5.81 | 349.23 | 4.07 | 310.75 |
| $S_2$ | 68.56 | 303.82 | 43.52 | 293.53 | 52.51 | 297.00 | 71.13 | 315.31 | 67.36 | 302.36 |
| $R_2$ | 2.00 | 282.50 | 0.45 | 327.25 | 1.06 | 273.76 | 4.28 | 283.66 | 1.44 | 277.51 |
| $K_2$ | 19.04 | 294.61 | 11.54 | 284.19 | 14.41 | 288.22 | 20.28 | 309.08 | 18.24 | 293.83 |
| $\eta_2$ | 1.12 | 328.73 | 0.63 | 301.12 | 0.95 | 305.03 | 1.42 | 7.92 | 0.97 | 323.09 |
| $2SM_2$ | 5.16 | 103.17 | 2.80 | 100.21 | 3.69 | 96.08 | 7.02 | 105.98 | 5.08 | 102.46 |
| $MQ_3$ | 0.76 | 151.31 | 0.46 | 130.37 | 0.35 | 153.78 | 1.18 | 116.99 | 0.72 | 149.97 |
| $MO_3$ | 1.98 | 174.82 | 1.17 | 152.32 | 0.87 | 148.27 | 2.62 | 127.98 | 2.02 | 170.68 |
| $M_3$ | 1.48 | 11.97 | 0.34 | 324.91 | 1.35 | 357.90 | 1.66 | 67.66 | 1.45 | 10.96 |
| $SO_3$ | 1.33 | 133.98 | 0.79 | 98.75 | 0.70 | 289.27 | 2.19 | 30.84 | 1.33 | 130.66 |
| $MK_4$ | 1.10 | 209.01 | 1.03 | 172.67 | 0.49 | 234.91 | 2.05 | 130.03 | 1.21 | 204.66 |
| $SP_3$ | 0.27 | 250.67 | 0.09 | 188.60 | 0.12 | 142.32 | 0.91 | 182.15 | 0.29 | 271.28 |
| $SK_3$ | 1.36 | 231.82 | 0.72 | 203.30 | 0.58 | 192.38 | 1.87 | 183.97 | 1.41 | 229.76 |
| $K_3$ | 0.20 | 197.71 | 0.17 | 178.53 | 0.19 | 210.49 | 0.62 | 149.23 | 0.23 | 211.07 |
| $MN_4$ | 0.38 | 5.49 | 0.96 | 201.55 | 0.82 | 37.20 | 2.99 | 105.02 | 0.30 | 353.84 |
| $M_4$ | 0.70 | 27.58 | 2.57 | 211.56 | 1.70 | 46.05 | 7.69 | 106.73 | 0.28 | 52.78 |
| $SN_4$ | 0.17 | 61.29 | 0.36 | 243.43 | 0.08 | 180.32 | 2.12 | 160.18 | 0.14 | 40.34 |
| $MS_4$ | 0.54 | 326.36 | 2.33 | 236.98 | 1.18 | 104.66 | 7.75 | 140.37 | 0.52 | 282.57 |
| $MK_4$ | 0.04 | 292.80 | 0.70 | 232.62 | 0.31 | 110.23 | 1.81 | 126.85 | 0.11 | 228.59 |
| $S_4$ | 0.34 | 50.69 | 0.51 | 267.57 | 0.06 | 109.52 | 2.73 | 187.81 | 0.25 | 37.96 |
| $SK_4$ | 0.13 | 40.33 | 0.23 | 273.76 | 0.06 | 156.02 | 1.25 | 175.92 | 0.06 | 10.88 |
| $M_6$ | 1.11 | 155.05 | 0.86 | 78.41 | 0.82 | 93.42 | 2.27 | 217.02 | 1.01 | 149.12 |
| $2MS_6$ | 1.46 | 180.29 | 1.23 | 104.10 | 1.21 | 111.22 | 3.05 | 238.90 | 1.39 | 173.03 |
| $2SM_6$ | 0.56 | 220.29 | 0.49 | 154.62 | 0.43 | 174.26 | 1.94 | 307.49 | 0.46 | 220.44 |

On the other hand, amplitudes of $(M_2+S_2)$ and $(K_1+O_1)$ are 163 cm and 43 cm respectively at Matsuai which is situated on the head of the bay: the former is about 3.8 times as large as the latter. Amplitude of $(M_2+S_2)$ at Matsuai is about 1.4 times as large as that at Akune, contrary to $(K_1+O_1)$ whose amplitude is nearly equal at both stations. $M_2$ and $S_2$ constituents in the bay have delayed angle of about 30° from the mouth to the Gannojiri-seto, and no more retardation over the inner bay. $K_1$ and $O_1$ constituents have delayed angle of only 10° from the mouth to the Gannojiri-seto.

Tide in the Bay of Yatsushiro seems to have notable overtides and compound tides like the tide in the Bay of Ariake, because the large tide range and the complex

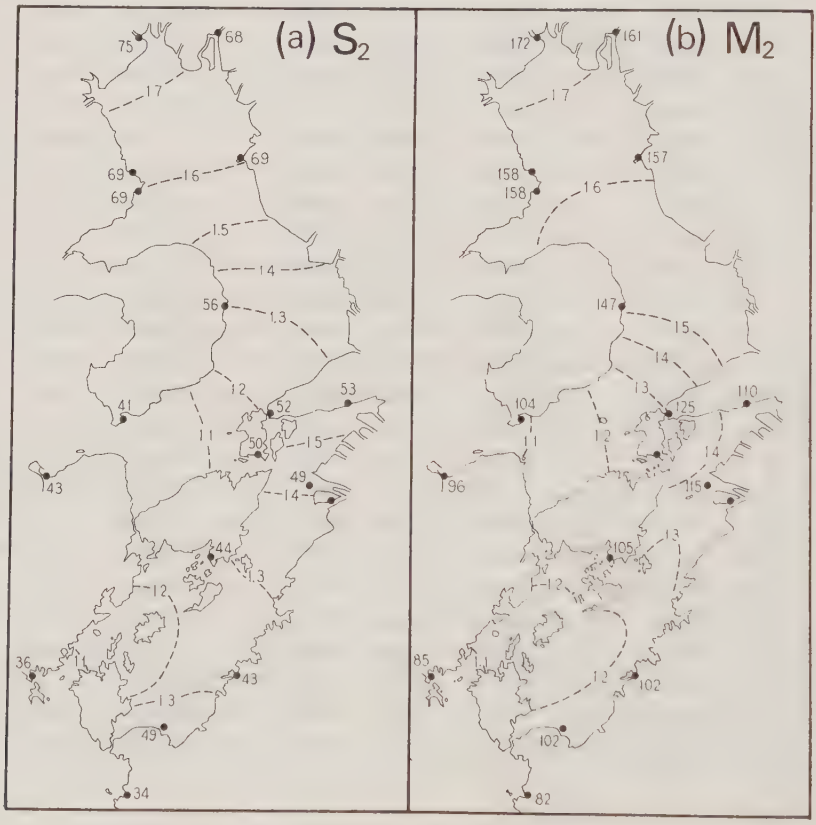


Fig. 3. Amplification factor of $S_2$ and $M_2$ constituents in the Bays of Ariake and Yatsushiro. Numerals near the location of respective stations show the amplitude of the constituents.

topography in the bay may excite remarkable nonlinear process in tidal oscillation. But we have not enough observations to understand detailed behavior of the tide in the bay.

Figs. 3a and b show distribution of observed amplitudes of $S_2$ and $M_2$ constituents relative to those outside the bays. Here the amplitudes at Tomioka and Akune are assumed to represent the tides outside the Bays of Ariake and Yatsushiro respectively.

In the Bay of Ariake, $M_2$ and $S_2$ constituents have the same relative amplitude of 1.7 at the bay head, but their distribution in the bay differs slightly from each other. That is, the relative amplitude of $M_2$ constituent has relatively large horizontal gradient from the bay mouth to the central part, and rather small gradient over the innermost region. On the other hand, the amplitude of $S_2$ increases almost linearly from the bay mouth to the bay head.

In the Bay of Yatsushiro, tidal waves invading the Nagashima Straits pass through the Hachiman-seto increasing their amplitude gradually, then enter the inner bay through Gannojiri-seto and Oh-seto and increase their amplitude toward south and north. Relative amplitude of $M_2$ constituent become 1.4 and 1.2 at the northern and southern ends of the bay respectively. The relative amplitude of $S_2$ constituent is 1.5 and 1.3 at the northern and southern ends respectively, which are somewhat larger than that of $M_2$ constituent.

Ogura (1933) attributed the large tidal amplitude in the Bay of Ariake to the mechanisms that semidiurnal tide is amplified by resonance with the proper oscillation of bay water, period of which is about 4 hours and has a ratio about 0.3 to semidiurnal tidal period, and that widespread shallow zone over the bay head may excite the amplification topographically. Diurnal tide has negligible amplification in the bay because the period of proper oscillation of the bay has a ratio about 0.15 to diurnal tidal period.

There is additional cause for the large tide range in these bays. Figs. 4a and 4b show the distribution of amplitude of $(K_1+O_1)$ and $(M_2+S_2)$ along the coast of the Japanese Islands to demonstrate local difference of tidal characteristics on the coast. In these figures the tide on the coast facing the Pacific Ocean and the East China Sea should be noted. Amplitude of $(K_1+O_1)$ is within 38~44 cm and local variability of it is rather small. On the other hand, amplitude of $(M_2+S_2)$ is about 41 cm on the coast of Hokkaido, increasing gradually toward southern coast, and reaches about 52 cm on the coast of the Kanto district, about 75 cm on the coast of Shikoku, and about 120 cm on the west coast of Kyushu which is about 3 times as large as that of

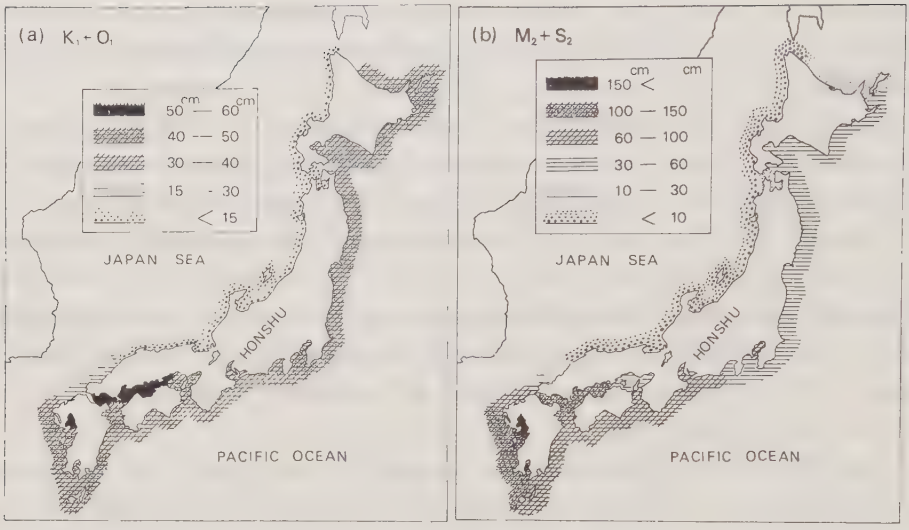


Fig. 4a, b. Distribution of $(K_1+O_1)$ and $(M_2+S_2)$ along the coast of Japanese Islands.

Hokkaido. Semidiurnal tide increases their amplitude in most bays on the Japanese coast except the Osaka Bay where the tide decreases remarkably, that is, the amplitude of $(M_2+S_2)$ reaches 76 cm in the Tokyo Bay, 100 cm in the Ise Bay, 144 cm in the Seto Inland Sea and 232 cm in the Bay of Ariake, but only 48 cm in the Osaka Bay.

Table 5 shows comparison of amplitudes of $(K_1+O_1)$ and $(M_2+S_2)$ at bay-head with those at bay-mouth for each of four Japanese representative bays. Principal diurnal tide does not amplify its range remarkably in any bays except for the Seto Inland Sea where the tide has an amplification factor of 1.386. On the other hand,

Table 5 Amplification of diurnal and semidiurnal tides in some representative bays in Japan.

| | Amplitude of $K_1+O_1$ | | Ratio | Amplitude of $M_2+S_2$ | | Ratio |
|---|---|---|---|---|---|---|
| | Bay mouth | Bay head | | Bay mouth | Bay head | |
| Bay of Tokyo | 40.13 cm (Mera) | 45.62 cm (Chiba) | 1.137 | 52.28 cm (Mera) | 75.69 cm (Chiba) | 1.448 |
| Ise Bay | 39.49 (Toba) | 43.38 (Nagoya) | 1.099 | 74.12 (Toba) | 100.42 (Nagoya) | 1.355 |
| Seto Inland Sea | 38.73 (Aburatsu) | 53.67 (Hiroshima) | 1.386 | 75.03 (Aburatsu) | 143.83 (Hiroshima) | 1.917 |
| Bay of Ariake | 47.0 (Tomioka) | 47.11 (Suminoe) | 1.002 | 139.00 (Tomioka) | 231.73 (Suminoe) | 1.667 |

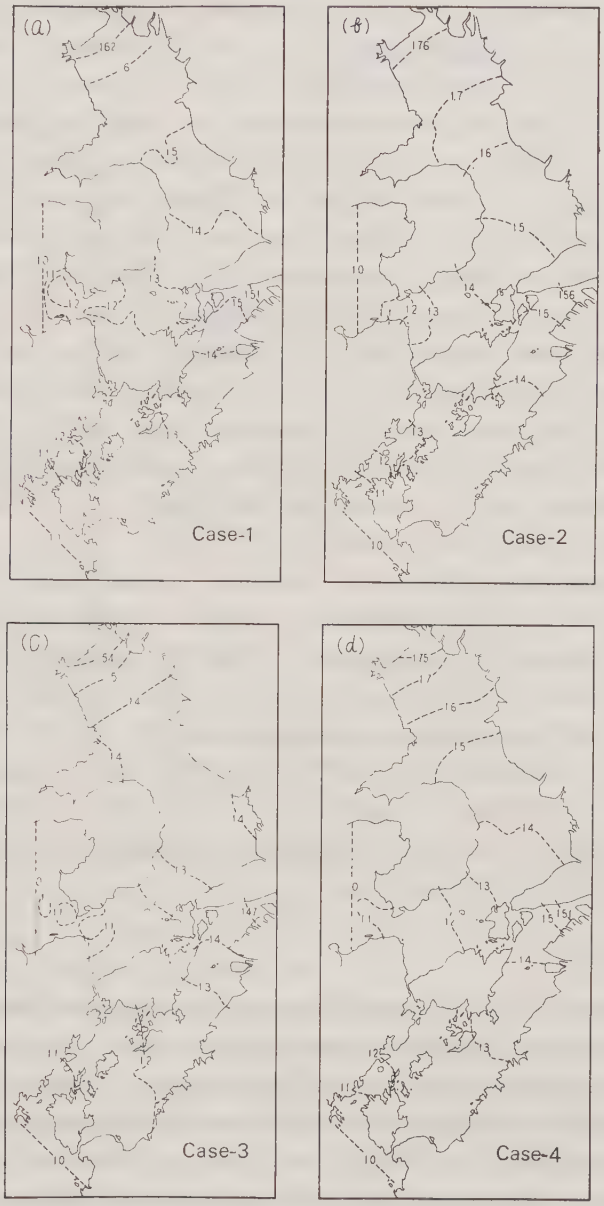


Figs. 5a–5d. Amplification factor of semidiurnal tide in the Bays of Ariake and Yatsushiro obtained from numerical experiments.

semidiurnal tide is amplified remarkably in every bay. The largest amplification factor is 1.917 in the Seto Inland Sea followed by 1.667 in the Bay of Ariake. Although the Seto Inland Sea has larger amplification factor of diurnal and semidiurnal tides than the Bay of Ariake, the former has smaller tide range than the latter. This fact is explained by the difference of the size of tide outside the respective bays. Namely, the large tide range in the Bay of Ariake is attributed to the large semidiurnal tide outside the bay in addition to remarkable amplification due to the resonant mechanism.

Figs. 5a–5b show amplitude of semidiurnal tide in the Bays of Ariake and Yatsushiro relative to those at Tomioka and Akune obtained by the four numerical experiments mentioned in the previous section. In the Bay of Ariake, the tide is amplified remarkably near the bay mouth and over the innermost part, and rather weakly over the central part. The largest relative amplitude at the bay head is 1.62 in spring tide and 1.76 in neap tide. When the tidal oscillation is associated with moderate wind its amplitude becomes larger or smaller than that in the case of no wind depending on the wind direction, from south or north.

The relative amplitude in the Bay of Yatsushiro increases linearly from the mouth to the head of the bay. The largest relative amplitude at the bay head is 1.51 and 1.56 in spring tide and neap tide respectively, which are somewhat smaller than those in the Bay of Ariake. When northerly moderate wind is blowing the amplitude becomes smaller than that in the case of no wind, but in the case of southerly moderate wind it is almost the same as that in the case of no wind. Generally, wind effect influencing the amplification of semidiurnal tide in the Bay of Yatsushiro is weaker than that in the Bay of Ariake. Distribution of tidal amplitude shown in Fig. 5 seems to agree reasonably with those in Fig. 3.

## 4. Tidal currents

The Hydrographic Office of Japan (1974) published charts of mean tidal currents in spring tide in the Bays of Ariake and Yatsushiro, based on the composition of a lot of tidal current observations taken in many occasions in the past several tens of years. The publication contains twelve charts corresponding to respective stages of the principal semidiurnal tide. Fig. 6 shows, as a representative example, a tidal current distribution corresponding to the tidal stage when the tidal currents have the fastest eastward flow at the Hayasaki Straits.

In the Bay of Ariake, the fastest flow of more than 7 knots is seen near the Hayasaki Straits. Strong current zone which has a speed of more than 2 knots covers from

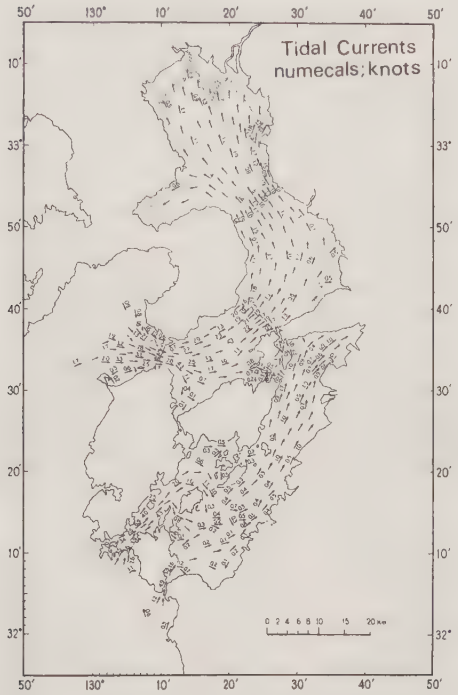


Fig. 6. Observed tidal currents in the case of spring tide at the stage when the flow reaches maximum through the Hayasaki Straits.

the bay mouth to the sea off Misumi. Over the northern area from the central part of the bay the currents are relatively weak, but a speed of more than 1 knot is still seen near the bay head. The currents flow parallel to the bay axis with maximum current zone close to the Shimabara Peninsula.

In the Bay of Yatsushiro, aspect of tidal currents is somewhat complex reflecting topographical complexity of the bay. The fastest currents of more than 6 knots are seen in the Nagashima Straits, and strong current zone which has a speed of more than 2 knots covers from the bay mouth to the Hachiman-seto. It is interesting that currents of more than 1 knot are seen near the northern end of the inner bay but the currents are less than 0.2 knots near the southern end. The formation of vast tide land near the northern ends of both bays may excite the tidal currents strongly.

In Figs. 7a–7d are shown representative examples of tidal current distribution which are obtained in the four experiments described in Section 2. They correspond to the

Figs. 7a–7d. Computed tidal currents at the stage when the flow reaches maximum through the Hayasaki Straits in cases of (a) spring tide with no wind, (b) neap tide with no wind, (c) spring tide with moderate north wind and (d) spring tide with moderate south wind.

stage when the tidal currents have the fastest eastward flow at the Hayasaki Straits. Currents presented here are given as a mean in 2 km square for vertically averaged values from the surface to the bottom.

In the Bay of Ariake, the fastest currents are seen near the Hayasaki Straits, which exceed 300 cm/s in spring tide either moderate wind blows or not. The currents in the bay decrease their speed toward the bay head, and are about 70–100 cm/s over the central part and 20–40 cm/s over the innermost part. The currents flow parallel to the bay axis, and the maximum current zone stretches close to the Shimabara Peninsula.

Maximum speed of tidal current through the Misumi-seto and Yanagi-seto is at most

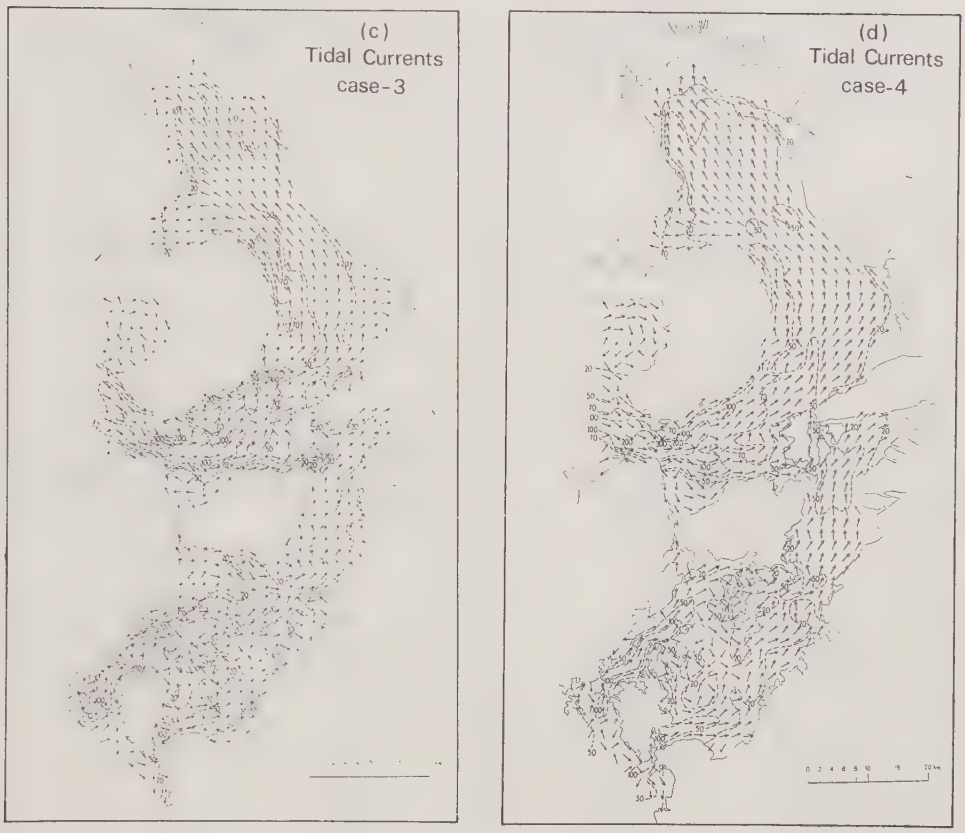


50 cm/s, and water volume passing through these straits is relatively small because of the narrow cross section of them. Such a condition weakens water exchange between the Bays of Ariake and Yatsushiro so as to isolate apparently these bays.

In the Bay of Yatsushiro, current speeds of 100 cm/s in spring tide and 50 cm/s in neap tide are seen over the Nagashima Straits and Hachiman-seto. The currents in the bay are about 20–50 cm/s and 10–20 cm/s in spring tide and neap tide respectively. The flow pattern in the case of no wind is distorted remarkably by moderate wind.

In comparison of Fig. 6 with Fig. 7, computed currents have generally somewhat slower speed than the observed currents, although the flow pattern of them resembles

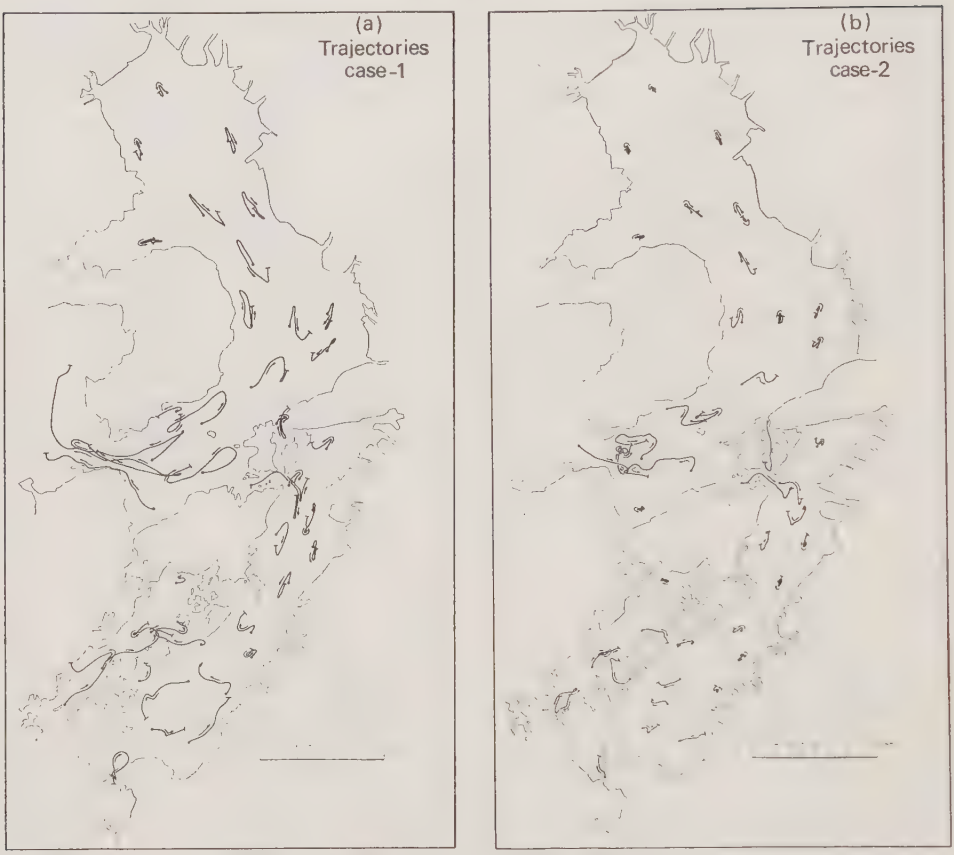


Figs. 8a–8d. Trajectories of water particles associated with tidal oscillation computed in cases of (a) spring tide with no wind, (b) neap tide with no wind, (c) spring tide with moderate north wind and (d) spring tide with moderate south wind.

each other. Especially, over the northern ends of both bays, observed currents have speeds about 2 times as large as those of computed one. This discrepancy may be due to the fact that the numerical model used here does not contain formation of tide land and inflow of fresh water which will increase the current speed locally.

Movement of water particles associated with periodic variation of tidal currents is examined by the trajectory analysis, in which the trajectories of water particles at 40 positions are constructed based on the computed currents. Figs. 8a–8d show the trajectories obtained under four conditions. Near the head of the Bay of Ariake, moving distance of water particles associated with the tidal variation is very small

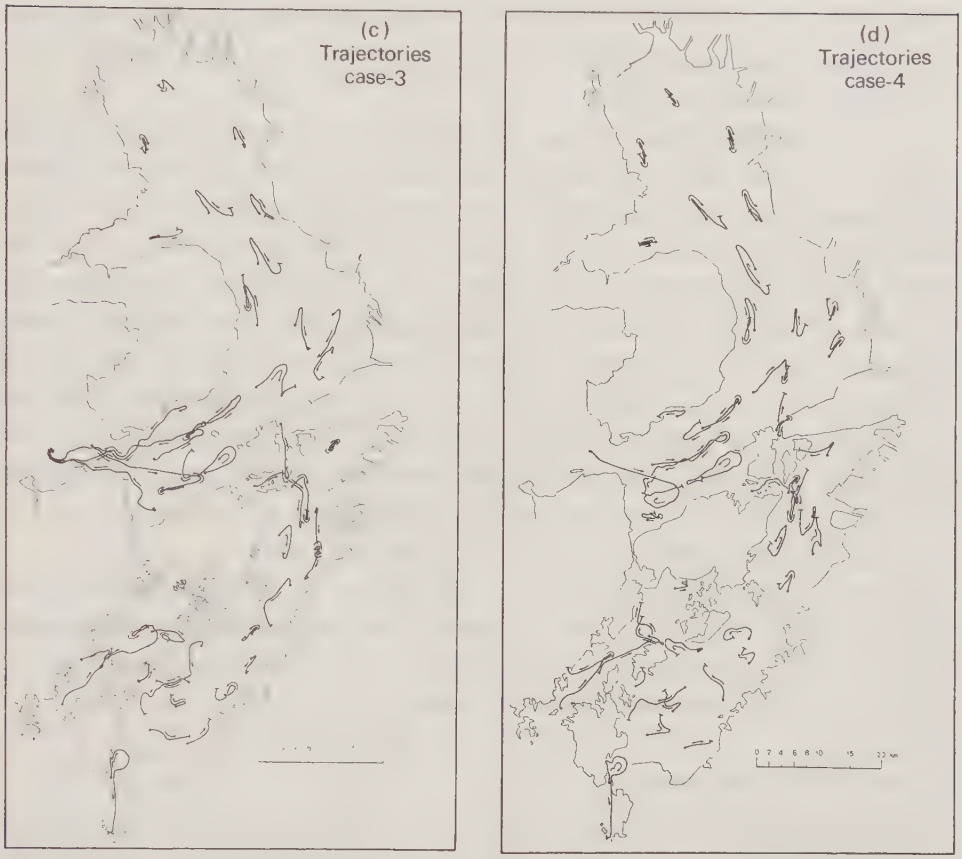


and about 2–6 km either moderate wind blows or not. But the distance may be practically longer than two times of these values because the observed currents have a speed more than two times as large as the computed currents.

Over the central part of the Bay of Ariake, moving distance of water particles is about 5–8 km and not be influenced by the moderate wind remarkably. Generally, water particles repeat the movement going ahead and back alternatively, but it will be seen by careful observation that the water is transported southward along the east coast and northward along the coast of the Shimabara Peninsula in the cases of no winds and moderate north wind as a resultant of periodic movement. In the case of

moderate south wind, is seen weak northward transport of bay water through whole cross section. The movement of water particles in neap tide is about one half as large as that in spring tide.

Very long moving distance of water particles is seen in southern part of the Bay of Ariake associated with tidal oscillation, especially it exceeds 20 km near and around the Hayasaki Straits. Respective trajectories differ largely in each of the four experiments, and it is concluded that the circulation of bay water caused by the tidal residuals in this area is influenced sensibly by wind and cannot have universal feature.

Over the Nagashima Straits and the Hachiman-seto in the Bay of Yatsushiro, water particles go and return periodically associated with tidal oscillation, and their moving distance is about 12 km and 5 km in spring tide and neap tide respectively. Over the northern part of the bay, water particles move repeating relatively regular south-north displacement in the case of no wind and their moving distance is about 6 km in spring tide. Net water mass transport toward south or north is seen as a resultant of periodic movement whether moderate north wind or south wind blows.

Over the southern part of the bay, moving distance of water particles associated with tidal oscillation is about 11 km and 4 km in spring tide and neap tide respectively. Curiously, movement of water particles in this zone is uni-directional and counterclockwise, and does not show periodic oscillation.

## 5. Tidal residual currents

Recently, circulation of bay water caused by the tidal residuals has been recognized to be as important as the behaviors of horizontal and vertical diffusion in the process of water exchange. Nagasaki Marine Observatory (1954) surmised a mean circulation in the Bay of Ariake based on the analysis of local oceanic conditions, in which sea water of outer ocean enters in the bay through southern part of the Hayasaki Straits and the bay water goes out through northern part of the straits after a counterclockwise circulation in the bay.

The Hydrographic Office of Japan (1974) also presented existence of a mean circulation of bay water based on the analysis of observed tidal residuals in a depth of 5 meters below sea surface as shown in Fig. 9. In this figure, plotted tidal residuals have large variabilities both in speed and direction, but a counterclockwise circulation and a clockwise circulation are seen in the northern part and the central part of the Bay of Ariake respectively. Tidal residual currents are very strong in the northern part of the Hayasaki Straits, having speeds of more than 0.8 knots toward outer ocean.

Fig. 9. Tidal residual currents estimated from observation of tidal currents.

Tidal residuals may be caused by wind stress acting on the sea surface, inflow of fresh water, topographical influence, nonlinearity in tidal motion, etc. Taking these causes into consideration it will be inferred that tidal residuals cannot organize a universal circulation pattern but reveal rather transient circulations. As an evidence, modification of tidal residual currents by wind stress acting on sea surface is examined through the present numerical experiment.

In the experiment, tidal residual current is defined at respective grid points as a vector mean of tidal currents averaged over one tidal period. Figs. 10a–10d show stream lines and equi-speed lines of tidal residual currents deduced from the values at respective grid points.

In the Bay of Ariake, tidal residual currents form themselves into three principal circulations which are situated on northern, central and southern parts of the bay, respectively. Over the northern part, the circulation is composed by a counterclockwise sub-circulation on the north off the Shimabara Peninsula and a clockwise sub-circulation on the innermost part of the bay in the cases of no wind and moderate

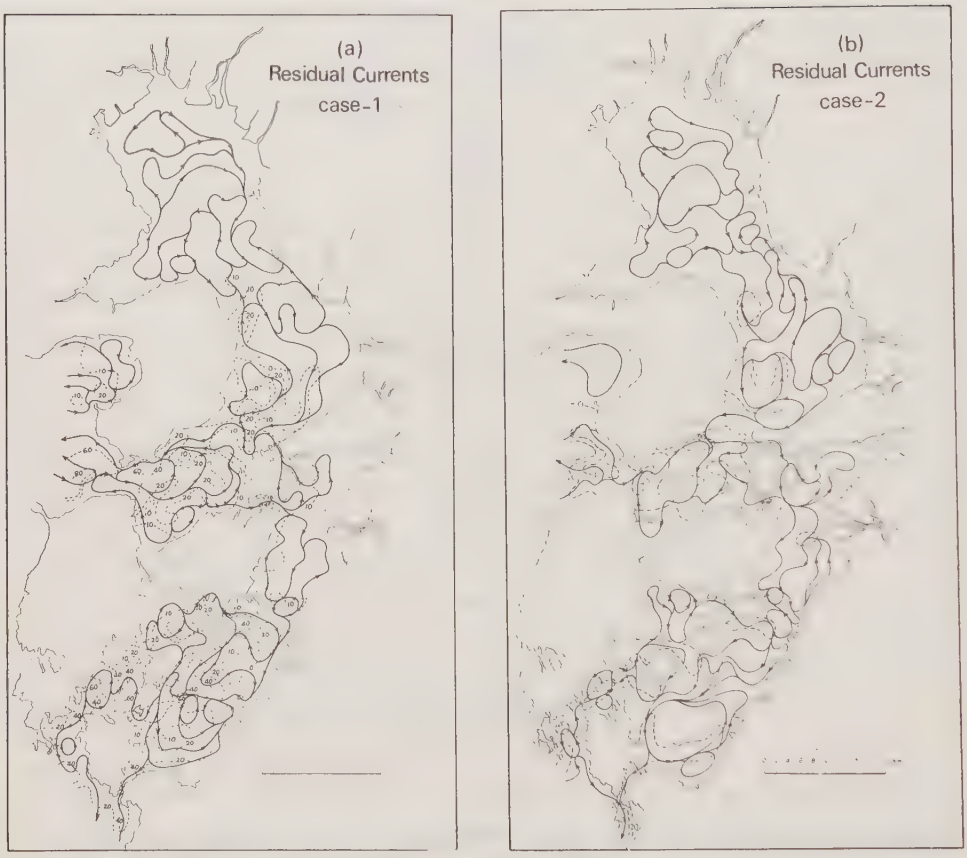


Figs. 10a–10d. Residual currents estimated from tidal computations in cases of (a) spring tide with no wind, (b) neap tide with no wind, (c) spring tide with moderate north wind and (d) spring tide with moderate south wind. Full curves are stream lines and broken curves the iso-speed lines.

northerly wind, and these sub-circulations reverse their senses in the case of moderate southerly wind. Speed of the residual currents is about 10 cm/s in spring tide.

Over the central part of the Bay of Ariake, southward currents are prevailing along the eastern coast in the cases of no wind and northerly wind contrary to the northward currents in the case of southerly wind. We can see remarkable northward currents off the northeast coast of Shimabara Peninsula either moderate wind blows or not. Speed of the residual currents over this area is about 10–20 cm/s in spring tide.

There is a large counterclockwise circulation of bay water in any cases of the

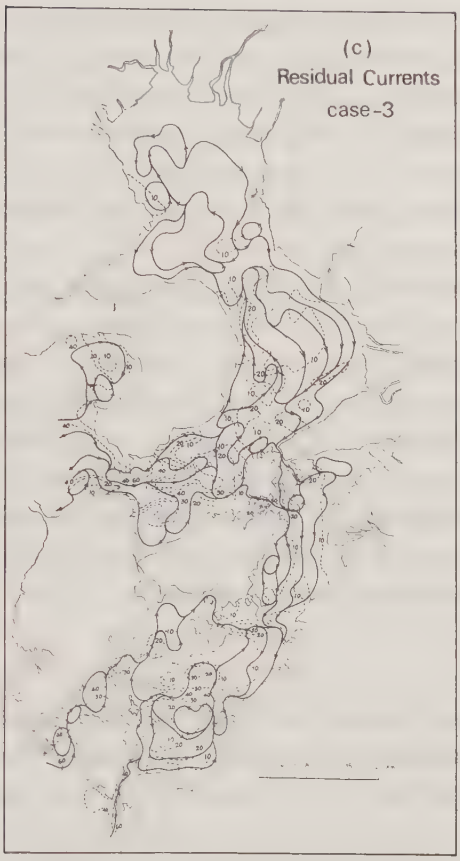


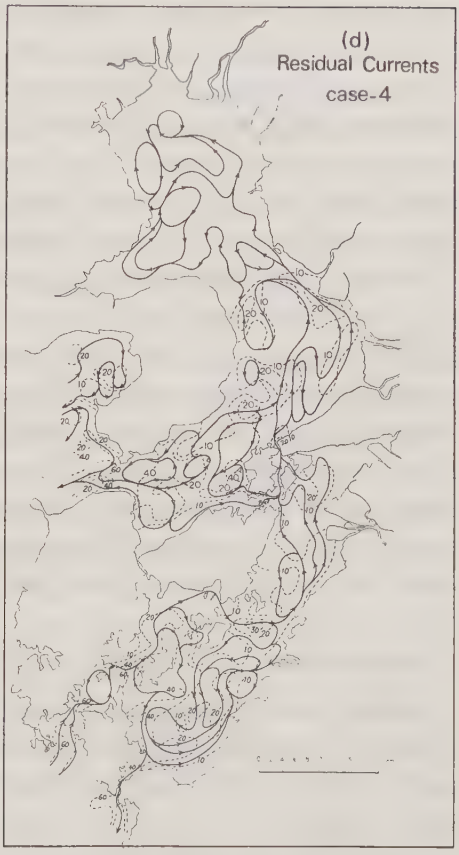


present experiments over the southern part of the bay. Speed of them is about 20–40 cm/s, and exceeds 60 cm/s near the bay mouth. The residual currents flow toward the Bay of Yatsushiro from the Bay of Ariake through the Yanagi-seto and toward the Bay of Ariake from the Bay of Yatsushiro through the Misumi-seto making counterclockwise circulation around Oyano Island in the case of no wind and moderate southerly wind. On the other hand, the residual currents flow toward the Bay of Yatsushiro through both straits in the case of moderate northerly wind.

There is a large clockwise circulation with a speed of about 20–40 cm/s in spring

tide in the Bay of Yatsushiro, where the currents enter the Bay of Yatsushiro through the Gannojiri-seto and the Oh-seto from the Hachiman-seto, and then return to the Hachiman-seto through the Mebuki-seto. Over the southern part of the inner bay, remarkable counterclockwise circulation is organized with a speed of about 20 cm/s in spring tide either moderate winds blow or not. Over the northern part of the bay the residual currents flow toward south or north with a speed of about 10–20 cm/s whether the direction of moderate winds is north or south.

Distributions of tidal residual currents obtained in the present experiments agree not so well with the flow pattern shown in Fig. 9 which was deduced from a composition of many observations. This finding might reflect that several assumptions and approximations for numerical model and accuracy of the tidal residual estimation are problematical. Namely, tidal residual currents are largely modified by moderate winds in the numerical experiments, while meteorological and oceanic conditions for respective tidal current observations used for estimation of tidal residuals are not well known. The above-mentioned disagreement suggests that refinement of the numerical model and accumulation of careful tidal observations should be necessary in future.

## 6. Mean sea level

Nagasaki Marine Observatory obtained mean sea level in the Bay of Ariake based on the tidal observation for a half of a month and levelling done at the same period, and showed interestingly that mean sea surface rises abruptly about 30 cm from the mouth of the bay to the central region of it, but ascent becomes gradual toward the bay head (Nagasaki Marine Observatory, 1954). Isozaki and Unoki (1964) showed in their numerical experiment of tide that the mean sea leve lin the Bay of Ariake increases from the entrance toward the central region and decreases gradually toward the north end, contrary to the observed result indicating gentle ascent. The maximum rising at the central region was about 19 cm above the level at the mouth in spring tide. They attributed the rise of mean sea level in the bay to the behavior of nonlinear terms contained in their numerical model.

Unoki and Isozaki (1965a, b) investigated effects of several factors such as bottom friction, meteorological elements, ununiform distribution of density of bay water, etc. which might have influence on the mean sea level in the bay, and concluded that the majority of conspicuous rise of mean sea level in the Bay of Ariake is attributed to the mean slope of sea surface of the second order due to the standing oscillation of tide.

In the previous numerical experiment (Isozaki and Unoki, 1964) computation was made over the Bay of Ariake, and tidal variation of sea level was given at the Hayasaki Straits as one of boundary conditions. It was also assumed that the Bay of Ariake does not connect with the Bay of Yatsushiro. In the present investigation, tidal numerical model is improved more or less, with fine mesh and large computation domain containing both of the Bays of Ariake and Yatsushiro. Tidal variation of sea level is given explicitly over the outer ocean as a boundary condition. Improvement of computation scheme mentioned above may produce different results especially in the mean sea level.

Figs. 11a–11d are the mean sea level obtained in the present experiment described in Section 2. It is very interesting that mean sea level descends remarkably on the Hayasaki Straits and its vicinity. In the case of no wind in spring tide, descent of mean sea level at the entrance of the Bay of Ariake reaches 15 cm, ascent of the level at the central region of the bay is 4 cm, and the difference of mean sea level between the entrance and the central region is 19 cm which agrees with the ascent of mean sea level at the central region in the previous experiment (Isozaki and Unoki, 1964). Gradual descent of mean sea level from the central region to the northern end of the bay is 3 cm which is about a half of the one in the previous experiment.

In the Bay of Yatsushiro variation of mean sea level is less than that in the Bay of Ariake, that is, descent of mean sea level in the Nagashima Straits is 3 cm and ascent of the level in the inner bay is 5 cm in the case of no wind in spring tide. In neap tide, variation of mean sea level is about one fourth of that in spring tide both in the Bays of Ariake and Yatsushiro.

Now consider the observed mean sea level at Kuchinotsu and Oura where tidal observation has been continued more than five years and levelling of tidal datum line has been done in recent years. Mean sea level averaged through recent 5 years at both stations are shown in Table 6 containing values for respective months. In the table mean sea level at Oura is higher than the level at Kuchinotsu, and the difference between both stations becomes larger in summer than in winter reflecting seasonal variation of sea water density, that is, the minimum difference is 4.9 cm of February, the maximum 10.3 cm, and yearly mean 7.4 cm. Although these values are much smaller than the value of 30 cm reported by Nagasaki Marine Observatory (1964), the discrepancy may be caused by difference of period length of tidal observation used. In the present numerical experiment difference of mean sea level between Kuchinotsu and Oura is 9.3 cm and 4.3 cm in spring tide and neap tide respectively,

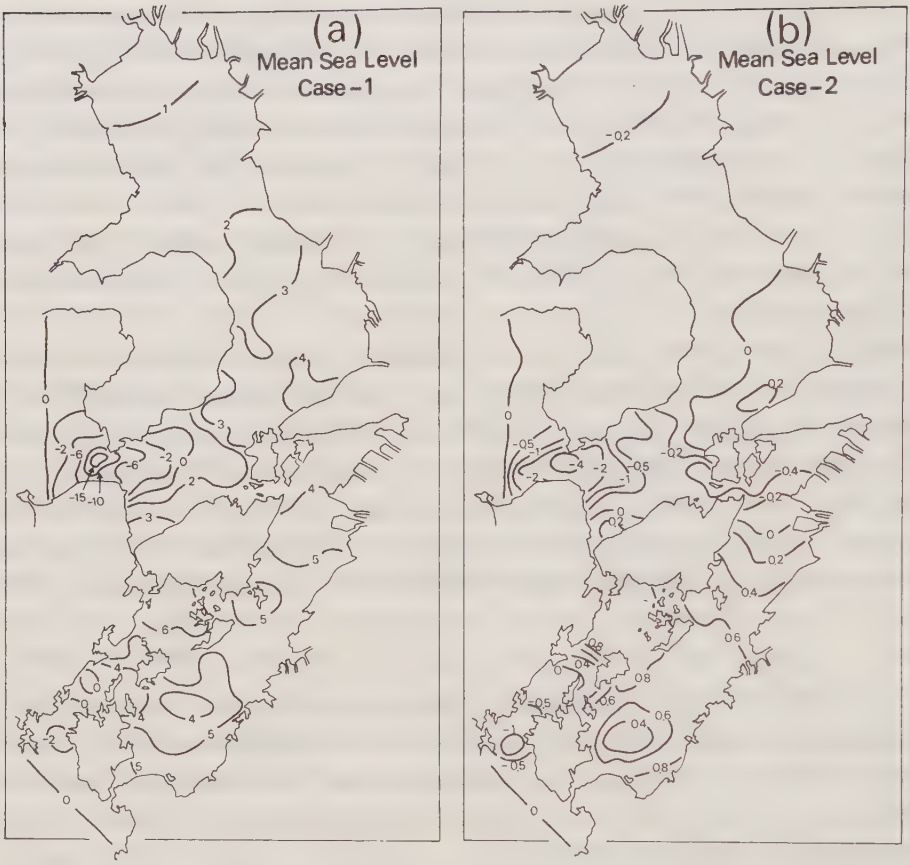


Figs. 11a–11d. Variation of mean sea level induced by the tidal oscillations computed in cases of (a) spring tide with no wind, (b) neap tide with no wind, (c) spring tide with moderate north wind and (d) spring tide with moderate south wind. (numerals: cm)

and the average of both values agrees reasonably well with the above-mentioned yearly mean difference obtained from the 5-year observations.

If the variation of mean sea level in both bays is attributed to the inclination of sea surface of the second order due to standing oscillation of tide, elevation of mean sea surface from still water, $\overline{\zeta}$, is given by

$$\overline{\zeta}+\frac{1}{2g}\overline{u^2}=\text{const.}, \tag{10}$$

where $\bar{u}$ is the current of water and $g$ the acceleration of gravity. We can easily

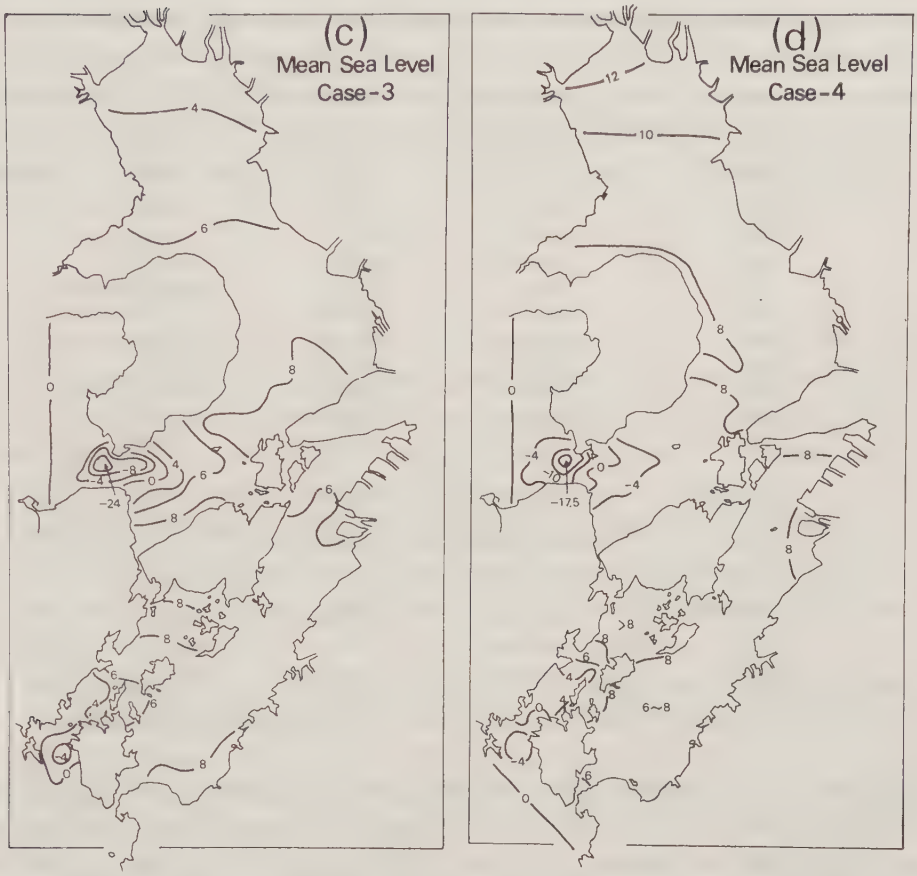


understand from Eq. (10) mean sea surface ascends in regions where the current is weak and descends in regions where it is strong, and the rate of mean sea level variation is proportional to the square of the current speed. This is the reason that the mean sea level descends remarkably in the Hayasaki Straits, and that the variation of mean sea level in neap tide is about one fourth of that in spring tide because the tidal current in the former case is about a half of the one in the latter case.

Southern coast of the Hayasaki Straits has higher mean sea level than the northern coast in any of the present experiments. The difference of mean sea level between

Table 6 5-year mean sea level above T. P. at Oura and Kuchinotsu.

| month | Oura | Kuchinotsu | Diff. |
|---|---|---|---|
| Jan | −0.150 m | −0.215 m | 0.065 m |
| Feb. | −0.192 | −0.241 | 0.049 |
| Mar. | −0.205 | −0.265 | 0.060 |
| Apr. | −0.115 | −0.183 | 0.068 |
| May | −0.001 | −0.074 | 0.073 |
| Jun. | +0.037 | −0.021 | 0.058 |
| Jul. | +0.146 | +0.043 | 0.103 |
| Aug. | +0.209 | +0.107 | 0.102 |
| Sep. | +0.171 | +0.079 | 0.092 |
| Oct. | +0.095 | +0.012 | 0.083 |
| Nov. | +0.019 | −0.095 | 0.076 |
| Dec. | −0.151 | −0.210 | 0.059 |
| mean | −0.015 | −0.088 | 0.074 |

(from Tide Tables for the Year 1975, JMA 1974)

| | | | |
|---|---|---|---|
| Spring tide | +0.013 m | −0.080 m | 0.093 m |
| Neap tide | −0.001 | −0.040 | 0.043 |

(Resuls of numerical tests)

both coasts is 5.3 cm and 1.3 cm in the cases of spring tide and neap tide respectively. This may be understood as a result of centrifugal force because the current is curved along the Shimabara Peninsula. Let radius of curvature of the current be $r$ and the mean speed of it $q=(\overline{u^2})^{1/2}$, then the difference of sea level between both sides of the straits with the breadth of $\Delta r$ is

$$\Delta\zeta = \frac{q^2 \cdot \Delta r}{gr} \tag{11}$$

In the case of the Hayasaki Straits, $q$ is about 150 cm/s in spring tide and 80 cm/s in neap tide, and $g=980$ cm/s$^2$; consequently,

$$\Delta\zeta = \begin{cases} 4.5 \text{ cm} & \text{in spring tide} \\ 1.3 \text{ cm} & \text{in neap tide} \end{cases} \tag{12}$$

which agrees reasonably well with the result of the numerical experiment.

In Case-3 and Case-4 in the present experiments which contain wind stress of moderate wind on the sea surface, descent of mean sea level at the bay mouth is

larger than that in the case of no wind. On the other hand, ascent of the sea level is excited near the bay head by the effect of wind set-up due to the shallowness there. Consequently, difference of mean sea level between bay mouth and bay had becomes notable and reaches 32 cm and 29 cm in the Bay of Ariake in Case-3 and Case-4 respectively. The values are similar to the one reported by Nagasaki Marine Observatory (1964).

## 7. Concluding remarks

In the present paper we tried to describe tidal phenomena in the Bays of Ariake and Yatsushiro systematically based on analysis of observed data and numerical experiment. Tide range, tidal currents, tidal residual currents and inclination of mean sea level in these bays were described. It is concluded that these are modified largely from the feature of astronomical tides by the meteorological effect such as wind stress in addition to nonlinear processes due to large tide range and complicated topography. Much more tidal observations are needed to understand complicated tidal phenomena in these bays systematically, together with the observations of meteorological elements, supply of fresh water from many rivers, and oceanic conditions.

Numerical experiment of tides was performed to supplement scanty observations, but the numerical model used here is not applied perfectly to local problems although it can give general situation of tide in a bay satisfactorily. Because, it does not contain fresh water inflow from rivers and formation of tide land, which will affect significantly the feature of tide over a shallow region.

As future problem, model experiment is desired in addition to the accumulation of tidal observation data and improvement of numerical tidal model.

## References

Hydrographic Office (1974): Tidal currents charts over the Bays of Ariake and Yatsushiro. Hydrographic Office, Japan, pp. 15.

Isozaki, I. and S. Unoki (1964): Computation of tides in the Bays of Tokyo and Ariake. Coastal Engineering in Japan, **7**, 125–131.

Miyazaki, M. (1967): Tidal constants along the coast of Japan. Oceanographic Magazine, **19**, 13–55.

Nagasaki Marine Observatory (1954): Oceanographic study concerning comprehensive development of Ariake Bay, Part I. Nagasaki Marine Observatory, pp. 76.

———— (1955): Oceanographic study concerning comprehensive development of Ariake Bay, Part II. Nagasaki Marine Observatory, pp. 123.

———— (1959): Research on the tidal phenomena in Ariake Bay by a hydraulic model (Part I). Journ. Meteorol. Res. JMA, **12**, 261–295.

———— (1961): Research on the tidal phenomena in Ariake Bay by a hydraulic model (Part II). Journ. Meteorol. Res. JMA, **13**, 83–100.
OGURA, S. (1933): The tide in the sea adjucent to Japan. The Bull. Hydrogr. Dept. Japan, **7**, 1–189.
SEKI, S. (1948): Tidal constants at Minamata in the Bay of Yatsushiro. Kenkyu Sokuho, **31**, 9–10.
UNOKI, S. and I. ISOZAKI (1965a): Mean sea level in bays, with special reference to the mean slope of sea surface due to the standing oscillation of tide. Oceanogr. Mag., **17**, 11–35.
———— (1965b): Proposed mechanisms on the inclination of mean sea level in a bay and the generation of surf beats. Proc. 12th Conf. Coastal Engineering, Japan, 7–13.

## 有明海と八代海の潮汐

磯崎一郎・北原栄子
（気象研究所）

明海有と八代海の潮汐変動は日本で最も顕著なもので，大潮時には有明海の湾奥で 500 cm を越える。この論文では潮汐観測資料の解析と数値実験にもとづいてこの特異な潮汐現象の実態を調べる。

潮差，潮流の特性，非線形効果から生ずる潮汐残差流，平均水面の傾斜などを論じ，さらにこれらが風によってどのように変形されるかを明らかにする。

これらの湾は比較的に浅くて広いために，非線形効果が顕著に現れること，及び気象の影響を大きく受けることが結論される。

The Oceanographical Magazine
Vol. 28, Nos, 1-2, pp. 33 to 45, March 1977

# Characteristics of Oceanographic Conditions in the Okhotsk Sea and Meteorological Conditions over the Far East in November

Masaomi Akagawa
*Hakodate Marine Observatory*

***Abstract***: The seasonal changes of oceanographic conditions in the Okhotsk Sea and meteorological conditions over the Far East advance rapidly or stepwise in the latter half of November.

Concerning the oceanographic conditions, the sudden drop of density of sea water along the Okhotsk coast of Hokkaidō, the rapid increase of density difference and the rapid decrease of sea level difference between the Japan Sea and the Okhotsk Sea, the retardation of falling of sea surface temperature of the Okhotsk Sea, and the passing enlargement of the Sōya Warm Current, etc., are noteworthy phenomena.

On the other hand, in November the deep atmospheric pressure trough forms near the Japan Islands and moving and deepening speeds are at the greatest; the frequent track of cyclones lies toward north in the middle part of November owing to the timely combination of the southward shift of polar jet stream and the expansion of the area of southerly component of geostrophic wind. Additionally, in the latter part of November, the 500 mb height difference between the Japan Sea and the Okhotsk Sea reaches its maximum, and in the same period the decrease of sea level pressure at Hokkaidō and the occurrence frequency of winter pressure pattern come to a standstill.

In this paper a discussion on the relations among these phenomena is given, and the uniqueness of the month of November in the seasonal change of oceanographic and meteorological conditions is emphasized.

## 1. Introduction

It is recognizable that change of season advances generally stepwise or discontinuously and a classification of season and the meaning of "Day of weather singularity" in climatology and meteorology have been discussed from such a point of view.

A November is ordinarily a turning point from autumn to winter in seasonal weather change and on the change of oceanographic conditions in the Okhotsk Sea also several interesting phenomena have been found in this month.

In this paper, characteristics of these changes are examined synthetically and on the uniqueness of a month of November a heavy emphasis is put.

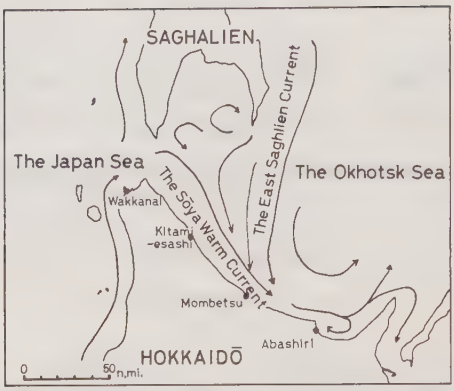


Fig. 1. Station locations and ocean current system.

Station locations and ocean current system relating to the coming discussions are shown in Fig. 1.

## 2. Change of oceanographic conditions

Oceanographic conditions of the Okhotsk Sea in cooling season have been investigated in relating to the study of sea ice. From the results of some investigations the following are noteworthy.

### 2.1 Sudden drop of the density of sea water on the Okhotsk coast of Hokkaidō

This phenomena occurs usually in November (Mean: 21st November) by the re-

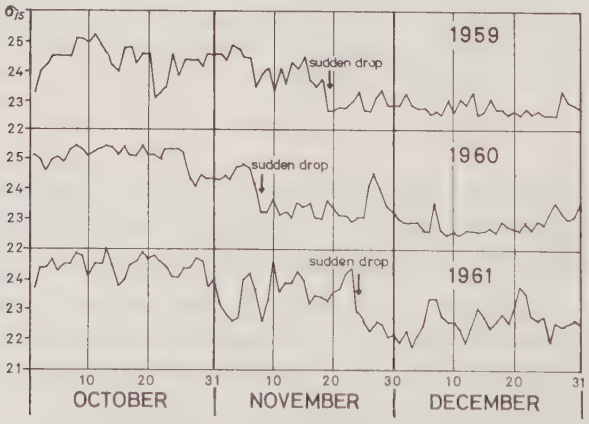


Fig. 2. Variation of daily $\sigma_{15}$ (specific gravity of sea water) at Mombetsu.

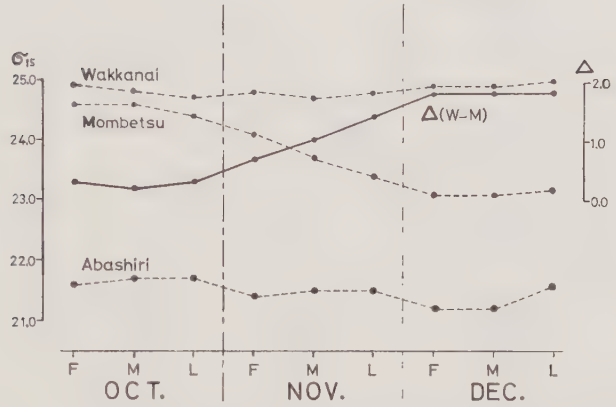


Fig. 3. Variations of the 10-day mean $\sigma_{15}$ during October to December at Wakkanai, Mombetsu and Abashiri, and the difference between Wakkanai and Mombetsu ($\Delta(W-M)$) (the 13-year (1956–1972) mean). F: the first ten-day of a month, M: the middle ten-day of a month, L: the last ten-day of a month

inforcement of the East Saghalien Current with low temperature and low salinity and it has been found that the date of the occurrence is correlated with the first date of pack ice appearance observed at the coast (Watanabe, 1963; Akagawa, 1967). Examples of the sudden drop at Mombetsu are shown in Fig. 2.

Further, on the examination of the 10-day mean $\sigma_{15}$ change during October to December at Wakkanai, Mombetsu and Abashiri shown in Fig. 3, it is evident that no change at Wakkanai, slow lowering at Abashiri and rapid lowering in November at Mombetsu are seen. Therefore, the difference of $\sigma_{15}$ between Wakkanai and Mombetsu becomes suddenly larger in November.

### 2.2 Retardation of falling of the sea surface temperature of the Okhotsk Sea

Akagawa (1968, 1972, 1975) pointed out that the retardation of falling of the sea surface temperature of the Okhotsk Sea occurs in the latter part of November and this phenomenon may be caused by such features of meteorological conditions as described later and the vertical structure of water temperature in the mixing layer, that is, the lower layer has somewhat warmer temperature. (Fig. 4)

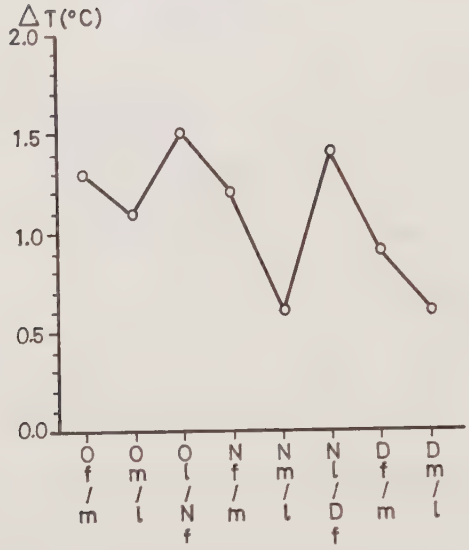


Fig. 4. Falling amounts of sea surface temperature every ten days in the Okhotsk Sea (the 11-year (1960–1970) mean).

### 2.3 Change of the difference of sea level between the Japan Sea and the Okhotsk Sea

Behavior of the Sōya Warm Current is said to be mainly due to the difference of sea level between the Japan Sea and the Okhotsk Sea. Iida (1969) indicated that the difference of the monthly mean sea level between Wakkanai and Abashiri reduces rapidly during November to December and suggested that a remarkable change of oceanographic condition occurs in the Okhotsk coast region of Hokkaidō in this period.

These changes by the 5-day mean sea level are shown in Fig. 5 and it is found that the normal change of the sea level in the period from October to December shows a gradual falling at Wakkanai and a gradual rising at Abashiri and the difference between the two stations becomes smaller suddenly after the middle part of November.

Generally speaking, a seasonal change of sea level is owing to rather meteorological and oceanographic conditions, i.e., atmospheric pressure, wind drift, sea water temperature and ocean current than astronomical tide.

Now, the normal changes from October to December of the sea level pressure at Wakkanai and Abashiri are +2.0 mb and −5.5 mb respectively. On the other hand,

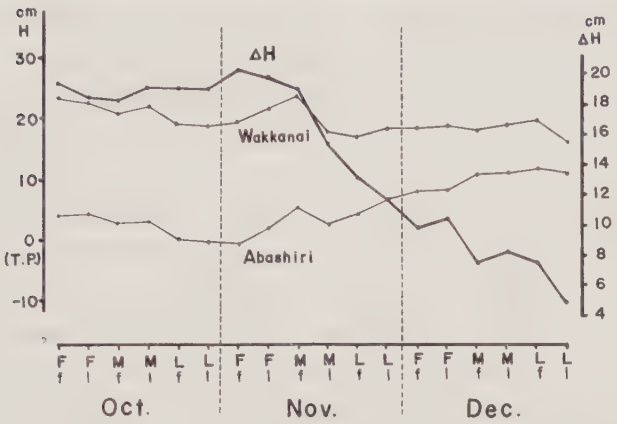


Fig. 5. Variations of the 5-day mean sea level during October to December at Wakkanai and Abashiri and the difference between the two stations ($\Delta H$) (the 15-year (1956–1970) mean).

the changes of the sea level at the two stations are −2.6 cm and +7.9 cm respectively. Judging only from the statical barometric factor, the change of the sea level at Abashiri is over the barometric effect, so that some effects of changes of oceanographic conditions in the Okhotsk Sea may be expected.

### 2.4 Passing enlargement of the Sōya Warm Current in November

Aota (1975) indicated that the sectional area of the Sōya Warm Current off Hokkaidō is at the maximum in August and then decreases rapidly, but in November the area shows a passing enlargement as seen in Fig. 6. He pointed out that it may be owing to a transitory increase of transport of the Sōya Warm Current though its mechanism is unknown.

### 2.5 Correlation between sea surface temperature and sea ice conditions in the Okhotsk Sea

The correlation coefficient between the sea surface temperature of the Okhotsk Sea and the first date of pack ice appearance along the coast of Hokkaidō falls temporally during the last part of November to the first part of December and conversely the coefficient between the sea surface temperature and the amount of ice along the coast in the same period becomes higher (Akagawa, 1975). In this respect it was suggested that the retardation of falling of the sea surface temperature in the latter

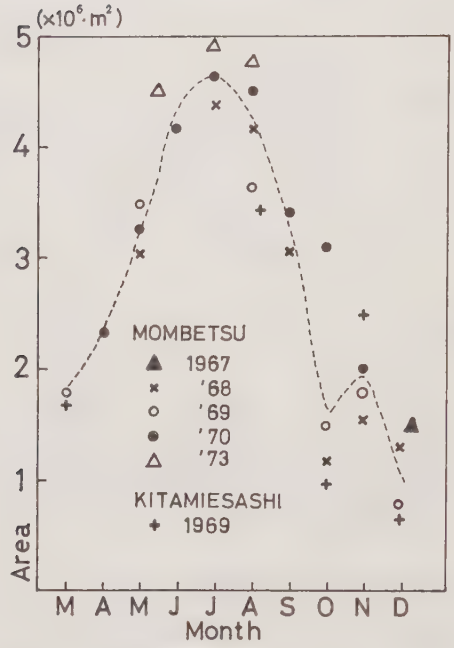


Fig. 6. Seasonal change of the sectional area of the Sōya Warm Current northeast off Mombetsu or Kitamiesashi in the period 1967–1970. (after Aota (1975))

part of November as mentioned in (2) will probably have something to do with this fact.

From arrangement of the above-mentioned facts, it may be accepted that usually in the latter half of November the oceanographic conditions of the Okhotsk Sea change suddenly due to the decay of the Sōya Warm Current, the reinforcement of the East Saghalien Current and the meteorological factors, and these changes contribute to the characterful changes of $\sigma_{15}$, sea level on the Okhotsk coast of Hokkaidō and water temperature in the Okhotsk Sea.

## 3. Characteristics of November viewed in the light of meteorological conditions

### 3.1 Atmospheric pressure field

On the characteristics of general circulation of the atmosphere during autumn to winter over Asia-Pacific area, it has been shown generally that trough over the Bering

Sea on the 500 mb height pattern moves westward rapidly in October~November, on the other hand trough over India region moves eastward and in November~December the two troughs unite near the Japan Islands forming remarkable trough from the high latitude to the middle (Katō, 1968; Yoshino, 1969).

Yoshino (1969) indicated that the movings of these troughs proceed stepwise and the combination of the troughs near 140°E line is formed towards the end of November, then winter pressure pattern becomes still more continuous. However, it is noticeable that change of occurrence frequency of winter pressure pattern advances stepwise and the middle part of November also is a stepped stage, as seen in Fig. 7 which shows the percentage frequencies every five days based on Yoshino's statistics. Considering an effect of cooling by winter monsoon, this stepped stage suggests the relation with the retardation of falling of sea surface temperature of the Okhotsk Sea mentioned above.

Fig. 8 shows the average of the 10-day mean sea level pressures at Wakkanai and Abashiri and the difference of the 5-day mean 500 mb height between the Japan Sea (40°N, 135°E) and the Okhotsk Sea (50°N, 150°E) in normal year.

The sea level pressure decreases rapidly in November, but a passing retardation of

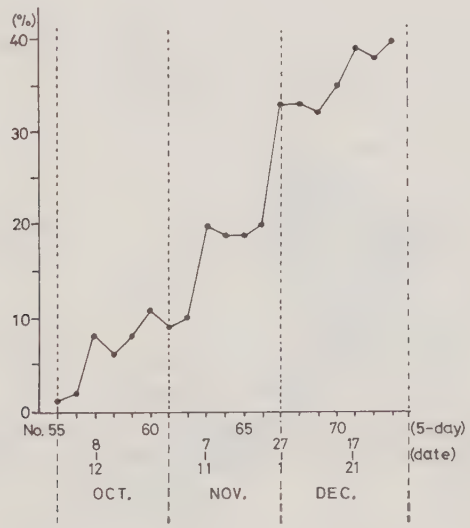


Fig. 7. Percentage frequencies every five days of the winter pressure pattern in the years 1907–1967. (after Yoshino (1969))

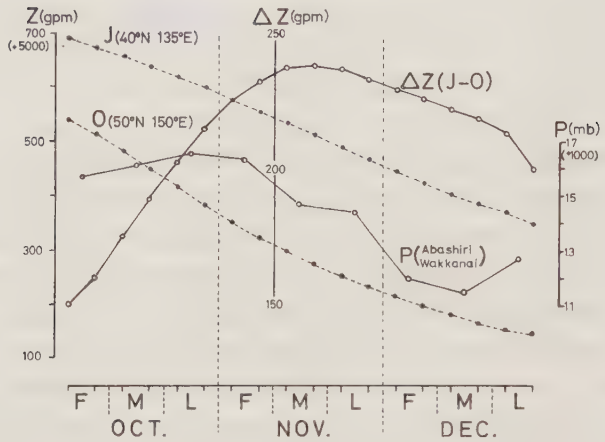


Fig. 8. The average of the 10-day mean sea level pressures at Wakkanai and Abashiri (P), and the 5-day mean 500 mb heights at the Japan Sea Point (40°N, 135°E) (J) and the Okhotsk Sea Point (50°N, 150°E) (O), and the difference between the two points ($\Delta Z$ ($J$–$O$)) in normal year.

Fig. 9. Types of the monthly mean sea level pressure change during October to December in the Far East.

the falling appears in the period from the middle to the last part of November. On the other hand, as seen in Fig. 9, normal change of the monthly mean sea level pressure during October to December in the Far East shows an increase over the

region west of about 135°E due to developing of the Siberian High, the highest in November over the region 135°E–140°E and a decrease over the region east of about 140°E due to developing of the Aleutian Low. Therefore, it is supposed that the retardation of sea level pressure change in November is due to the result of counter-balance of the three types of atmospheric pressure change mentioned above.

The difference of the 5-day mean 500 mb height between the Japan Sea and the Okhotsk Sea increases rapidly in October and amounts to the maximum in the middle of November. This phenomenon corresponds with a rapid extending of pressure trough from the polar region to the Okhotsk Sea in November.

### 3.2 Behavior of cyclone

It is known that both moving and deepening speeds of cyclone near the Japan Islands are at the greatest in November on the average (Takahashi, 1955, 1969).

On the frequent track of cyclone over the Okhotsk Sea, Akagawa (1968) pointed out that cyclones in the middle part of November pass mostly over the northern or the central part of the sea, but in the first and the last parts of November they pass over the southern part of the sea. Here, Fig. 10 shows the prevailing tracks of cyclones every ten days in cooling season from the data in the years 1960–1970.

Axis of polar jet stream over the Far East normally shifts to south during summer to winter, on the other hand southerly component of geostrophic wind on the 500 mb surface becomes stronger and wider over the Pacific-Okhotsk sea area in the same

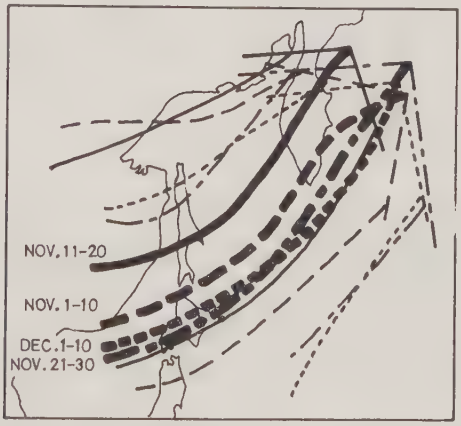


Fig. 10. Prevailing tracks of cyclones every ten days in cooling season in the years 1960–1970.

season (Katō, 1968). Therefore, it is supposed that this tendency of northern track of cyclone in the middle part of November will be attributed to the result of timely combination of the two current patterns.

From the facts mentioned above, it is to be emphasized that a month of November has peculiar features also on the seasonal change of meteorological phenomena in the Far East. Namias (1952) also stated that on the character of month to month persistence in climatic anomalies, air temperature, precipitation and the 700 mb height are usually conservative, but the relation of October to November has no continuity or it is rather apt to turn.

## 4. Discussion and Summary

In the above sections, it has been pointed out that both features of oceanographic conditions in the Okhotsk Sea and meteorological conditions over the Far East in November are very peculiar and seasonal changes occur rapidly or discontinuously having a stepped stage of the latter part of November.

Atmospheric pressure troughs on the 500 mb height pattern reach rapidly near the Japan Islands in November forming a polar front and activity of cyclone increases. Whenever cyclon passes, winter pressure pattern prevails, therefore seasonal change from autumn to winter advances stepwise.

By the outbreaks of winter monsoon, the southward flow of the East Saghalien Current in the Okhotsk Sea is reinforced and the low density water rapidly extends to Hokkaidō, consequently the sudden drop of density of sea water is observed on the coast. In this season the Sōya Warm Current decays due to the rapid decrease of difference of sea level between the Japan Sea and the Okhotsk Sea, which is caused by a rising of sea level in the Okhotsk Sea and a falling in the Japan Sea owing to the change atmospheric pressure pattern besides the extension of the low density water.

Cyclones taking south track over the Okhotsk Sea in the first and the last parts of November compared with the north track in the middle part are apt to bring cold air and strong wind to the Okhotsk Sea owing to the structure what is called "Cold Low", therefore the falling of sea surface temperature in the latter part of November becomes slower comparatively further under the effect of a slum in monsoon activity in the same period.

Fig. 11 shows the inter-annual variations of the dates of $\sigma_{15}$ sudden drop ($D\sigma$) at Mombetsu, sudden decrease of the sea level difference between Wakkanai and Abashiri

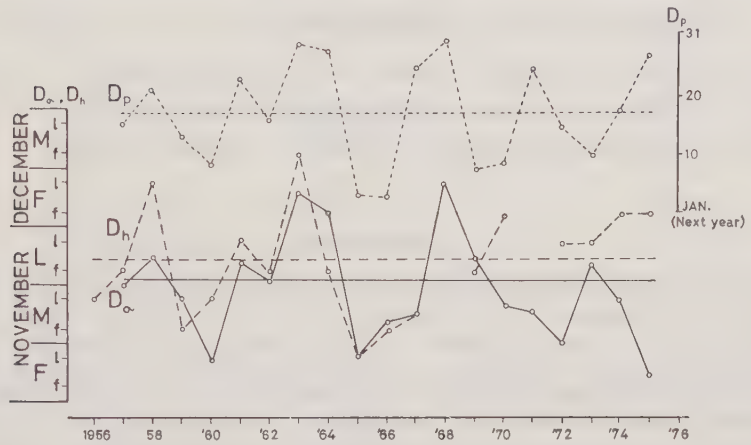


Fig. 11. Inter-annual variations of the dates of $\sigma_{15}$ sudden drop at Mombetsu ($D_\sigma$), sudden decrease of the sea level difference between Wakkanai and Abashiri ($D_h$) and the first appearance of pack ice at Mombetsu ($D_p$).

($D_h$) and the first appearance of pack ice at Mombetsu ($D_p$). It is seen that the trends of these three variations are roughly alike each other. As the East Saghalien Current promotes the growth of sea ice in the Okhotsk Sea and transports pack ice to the coast of Hokkaidō, some significant correlations among the three phenomena should be expected; in fact, the correlation coefficient between $D\sigma$ and $D_p$ is 0.688 for the years 1957–1973 and the one between $D\sigma$ and $D_h$ is 0.422 for the years 1957–1975.

However, it is noticeable that since 1970 the correlations have become lower or inverse; it may be caused by the change of observational environment due to the improvement of Mombetsu Port.

Additionally, features of November have been considered a important factor on the long-range forecasting for summer weather in North Japan. Matsukura (1969, 1971) suggested that the characteristic general circulation pattern which yields a cold or a hot summer doesn't appear accidentally and the circulation pattern in the previous autumn season shows a precuisive features of which strength and continuity relate to the occurrence of the circulation pattern yielding a cold or a hot summer.

In conclusion, it is summarized that both the oceanographic conditions in the Okhotsk Sea and the meteorological conditions over the Far East change very peculiarly, even dramatically, in November by the interactive processes and the uniqueness of a month of November should be emphasized.

**Acknowledgments**

The author wishes to express his hearty thanks to Dr. H. Wada of the Hakodate Marine Observatory for constant encouragement. Thanks are also due to Dr. H. Matsukura of the Japan Meteorological Agency for valuable discussion.

**References**

AOTA, M. (1975): Studies on the Sōya Warm Current. Low Temperature Science, Ser. A. 33, 151–172. (in Japanese)

AKAGAWA, M. (1967): Practical Method for Long Range Sea Ice Forecasting. Technical Report of the Japan Meteorological Agency, No. 59, 85–118. (in Japanese)

———— (1968): The Mean Sea Surface Temperature of the Okhotsk Sea in Cooling Season (Preliminary Report). Records of Oceanographic Works in Japan, **9** (2), 263–278.

———— (1972): The Mean Sea Surface Temperature of the Okhotsk Sea in Cooling Season (Second Report). Oceanogr. Mag., **24** (1), 57–63.

———— (1975): Relations between Oceanographic Conditions and Sea Ice in the Okhotsk Sea. Reports of Special Studies on Sea Ice Disaster by the Science and Technology Agency, 159–174. (in Japanese)

IIDA, H. (1969): Oceanographic Conditions of the Okhotsk Sea. Kishō Kenkyū Note (Meteorological Study Note), No. 101, 480–491. (in Japanese)

KATŌ, H. (1968): Annual Variations of Monthly Normal Fields of Basic Meteorological Elements. Jour. Meteor. Research, **20** (11), 581–609. (in Japanese)

MATSUKURA, H. (1969): Long-range Forecasting for Next Warm Season Weather by Features of General Circulation in Autumn Season. Tōhoku-Chihō Chōki-Yohō Sokuhō (Bulletin of Long-range Forecast for the Tohoku District), **21** (2), 7–18. (in Japanese)

———— (1971): Long-range Forecasting for Occurrence of Cold Summer in North Japan. Manual of Seasonal Weather Forecasting in Japan by the Japan Meteorological Agency, Vol. 2, 325–356. (in Japanese)

NAMIAS, J. (1952): The annual course of month to month persistence in climatic anomalies. Bull. Amer. Meteor. Soc., **33**, 279–285.

TAKAHASHI, K. (1955): Dō-Kikō Gaku (Dynamic Climatology). Iwanami-Shoten, Tokyo, pp. 316. (in Japanese)

———— (1969): Sōkan-Kishō Gaku (Synoptic Meteorology). Iwanami-Shoten, Tokyo, pp. 385. (in Japanese)

YOSHINO, M. (1969): On the Occurrence Frequency of Winter Pressure Pattern and its Relation to the 500 mb Level Characteristics. Tenki (Weather), **16** (1), 30–36. (in Japanese)

WATANABE, Kn. (1963): On the Reinforcement of the East Saghalien Current preceding to the Sea Ice Season off the Coast of Hokkaidō. Oceanogr. Mag., **14** (2), 117–130.

Characteristics of Oceanographic Conditions in the Okhotsk Sea

# 11月におけるオホーツク海の海況および極東域の気象の特徴

赤川正臣
（函館海洋気象台）

オホーツク海の海況や極東域の気象の季節変化は，おおむね11月中～下旬に，急激にあるいは階段的に起こり，非常に特徴的な様相を示すことが調べられた。

海況変化については，北海道オホーツク海沿岸における海水比重の急落，日本海側とオホーツク海側との比重差急増・水位差急減，オホーツク海海面水温降下の鈍化，宗谷暖流の一時的回復，水温と海氷現象との相関場における変化などがある。

一方，気象の方では，11月ころに日本附近で深い気圧の谷が形成され，低気圧の移動・発達の速度が最大となり，ポーラー・ジェットの南下と地衡風南分の増大との時間的かねあいに由ると思われる11月中旬のオホーツク海低気圧経路の北偏傾向がみられる。また，日本海とオホーツク海の500mb面高度差は11月中旬後半が最大で，北海道（稚内，網走）の海面気圧は中～下旬にその降下が鈍り，同時期に冬型気圧配置出現頻度の中だるみ（階段的変化）もみられる。

この論文では，これら現象間の関連，総合的結びつきが議論され，海況・気象の季節変化における11月という月の特異性が強調されている。

The Oceanographical Magazine
Vol. 28, Nos. 1-2, pp. 47 to 58, March 1977

# Visual Wave Observations on Board the R/V Keifu-maru

Takaaki Kimura*

***Abstract*:** Evident characteristics of the data which were obtained in these visual wave observations are presented separately after the observational elements, namely.

(1) *Wind-wave height*

When cruising, observers have a tendency to obtain data of the wind-wave height 5–10% higher when the waves are coming from the stem and 10–20% lower when they come from the stern.

Moreover, unskilled observers have a tendency to obtain them 5–20% lower than those of the skilled observers.

(2) *Swell height*

When swells are not distinguishable because of the predominant wind-waves, unskilled observers have a tendency to measure swell height 5–20% lower than those of the skilled observers.

(3) *Scattering of the observational data*

It is clarified that the measurements of those elements show unexpected wide scattering.

Such results will be useful for making the Ocean Wave Chart.

## 1. Introduction

The facsimile broadcasting of the Ocean Wave Charts (once a day) which are made by Marine Department of Japan Meteorological Agency came into operation since January 1972. All wave data which were put to use for making the charts are being obtained mainly by visual wave observations on board the research vessels or merchant ships. Recently, JMA has been developing ocean wavemeters to improve the quality of ocean wave measurements and we have been testing such wavemeters on board the Keifu-maru.

From weather charts we have been often obtaining the different wave data from two ships which were located almost at the same site and under the similar weather conditions. Theoretically speaking, these data from these two ships should be almost identical. The reasons of these discrepancy should be as follows:

(1) Difference of sailing state**

* Marine Department, JMA

** The majority of the observational data of merchant ships are obtained in sailing.

(at head waves, lee waves and stopping)

(2) Difference of observational positions

a: Difference of observational sides

(wave coming side or leaving side)

b: Difference of the height from the sea level

(3) Difference of the skill of visual wave observers

Visual wave observational data of merchant ships are only basic data to know actual sea state and their accuracy relates to the above-mentioned factors. Therefore, comprehensive investigation about these factors of visual wave observational accuracy is important.

We investigate the relation of the state of ship and the various modes of visual wave observations, on board the Keifu-maru in the vicinity of Izuoshima Island in April 1974. The results of the investigation are mentioned in this report.

## 2. The observational method

These visual wave observations were carried out in three different times A, B and C. A was 14:00–15:00 April 26th; B, 13:30–14:30 April 29th and C, 14:00–15:00 May 1st. The sea state of each observation were different. Wind-wave height was 1 m, swell height was 2 m at the time of observation A, both heights were 3 m at the B and both heights were 1–1.5 m at the C, respectively.

The Ocean Wave Charts at the days of the observations are shown in Fig. 1 and the sequence of wind direction and speed at the Keifu-maru are shown starting about 16 hours in advance in Fig. 2.

In each observational time A, B and C, the first observations were taken on sailing in a head and were named A-1, B-1 and C-1, and the second on sailing in a lee were named A-2, B-2 and C-2, and the third on stopping were named A-3, B-3 and C-3, respectively. Therefore, a total of them were nine times. The sailing state is shown in the circular figures of the right side of Fig. 4 with the *in situ* distribution of swell direction.

As shown in Fig. 3, the observational positions on board were nine and we stationed two observers* to each position.

We took account of the following conditions in stationing the observers.

(1) One observer measure waves for only once at the same post.

(2) He will not continue to observe at the same post (deck).

* At only one position, one observer was stationed.

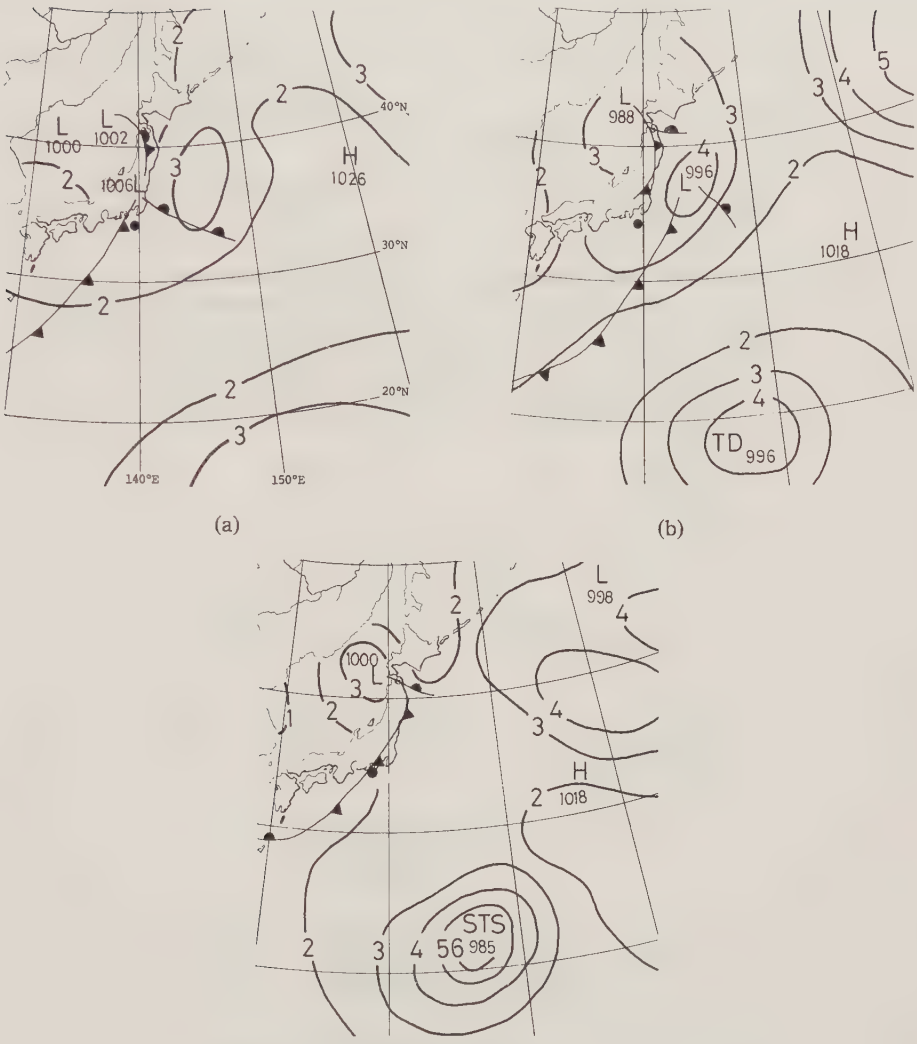


Fig. 1. Ocean Wave Chart

The unit of significant wave height is in metre.

Location of the Keifu-maru is shown with a black circle.

(a) 09I (JST), Apr., 26th, 1974
(b) 09I, Apr., 29th, 1974
(c) 09I, May, 1st, 1974

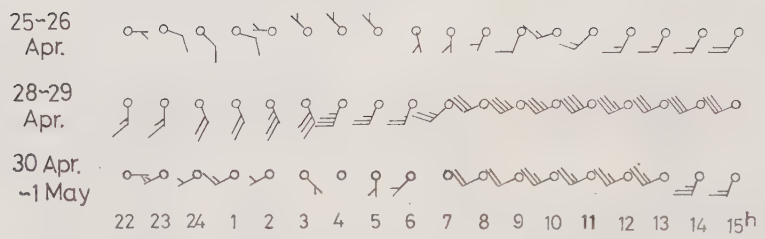


Fig. 2. Wind direction and speed taken on board the Keifu-maru
She was at the location 15 nautical miles south-east of Izuoshima Is. in the days of April 25–26th, 28–29th and then at the outer region of Ito-harbour in the days from April 30th to 13I (JST), May, 1st, and then at the entrance of Suruga-bay since 14I in the same day.
All visual observations were taken between 14I and 15I.

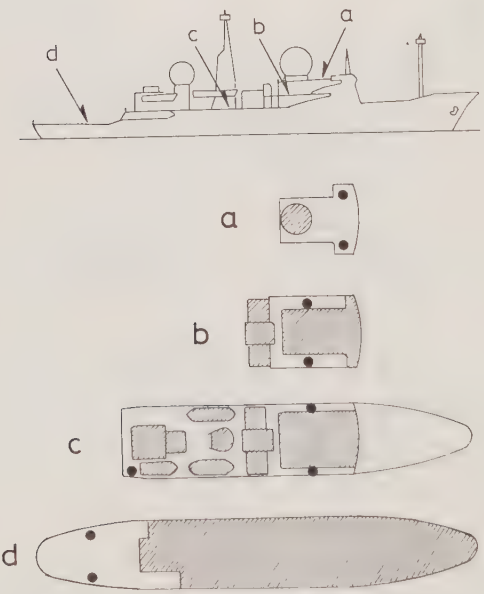


Fig. 3. The station of observers (shown by black circles)
a: Compass BR. Deck (9.5 m height from the sea level)
b: Navigation BR. Deck (7.0 m height)
c: F'CLE Deck (4.5 m height)
d: Upper Deck (2.5 m height)

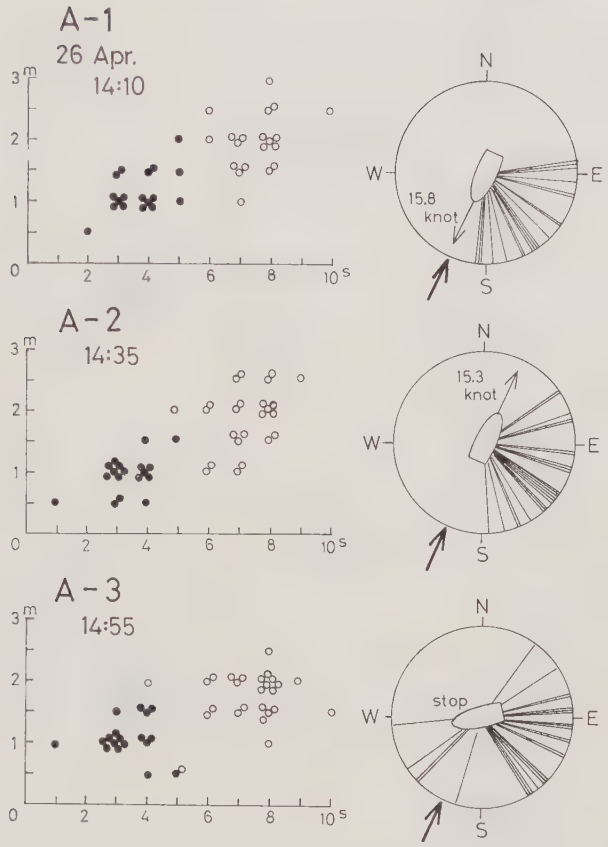


(a)

Fig. 4(a, b, c). The data distribution of wind-waves and swells and the sailing state

The abscissa is wave period (sec) and ordinate is wave height (m), the black points show wind-wave data and the white points show swell data. The circular figures at the right side show the distribution of visual swell coming direction and a sailing state (the bow direction and speed), and the bold arrows out of the circles show the wind-wave direction.

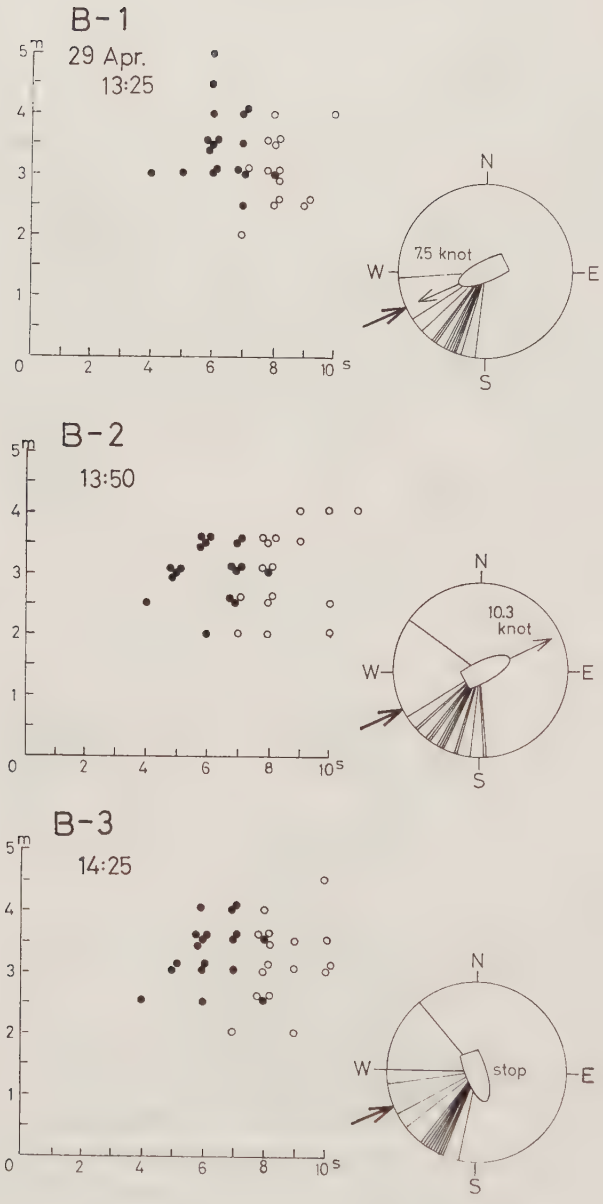


(b)

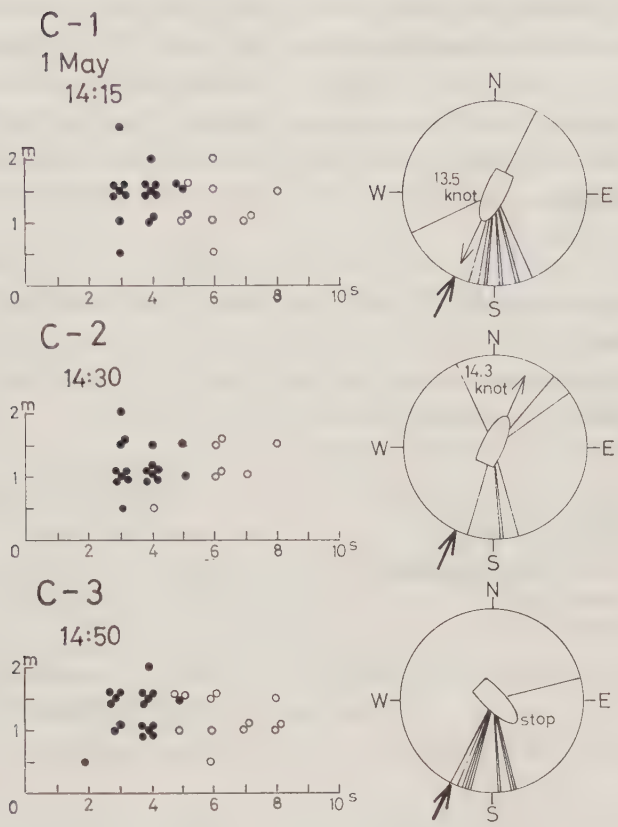


(c)

(3) We divide observers into two groups* according to the degree of visual wave observational experience, and the two observers at the same post are composed of superior and less superior ones.

Wave heights were measured in 0.5 metre steps, in 1 second steps for wave period. Wave directions were measured in increments of 10 degrees with bow direction as reference (0°).

Fig. 4 shows all the observational data** of these visual wave observational series

* The skilled group has the experience of the maritime observations either on board the Keifu-maru or Ocean Weather Ships for long time, and the unskilled group has less experience.

** The data of the seaman who was watching at the navigation bridge were added to those of the seventeen observers which were stationed at nine positions. Those data were included in Table 1 and in Table 4 (unskilled group).

A, B and C, and they are wave height, period and direction, respectively. At the observation A*, a few observers obtained the swells of two series. In this case, we expected the separate observations of swell directions, but it is difficult to discriminate the series exactly by visual observations. Therefore, in this investigation, when there are two swells from different directions, we adopted only one having larger wave height, and when the wave heights are identical, we adopted the one having larger period.

### 3. The characteristics of the visual observational data reflecting the difference of sailing state

Table 1 shows the average and variance of the period and height of wind-waves and swells which were obtained from the nine observations.

Table 1. The average and variance of each observational data
Left: The number of data
Center: The average (period: sec, height: m)
Right: The variance

| | | A | | | B | | | C | |
|---|---|---|---|---|---|---|---|---|---|
| Wind-wave period | 1 | 18 | 3.7 | 0.71 | 18 | 6.3 | 0.80 | 18 | 3.7 | 0.47 |
| | 2 | 18 | 3.4 | 0.72 | 18 | 6.2 | 1.09 | 18 | 3.6 | 0.49 |
| | 3 | 18 | 3.4 | 0.72 | 18 | 6.3 | 1.04 | 18 | 3.6 | 0.49 |
| Wind-wave height | 1 | 18 | 1.2 | 0.12 | 18 | 3.5 | 0.40 | 18 | 1.4 | 0.17 |
| | 2 | 18 | 0.9 | 0.09 | 18 | 3.0 | 0.19 | 18 | 1.1 | 0.11 |
| | 3 | 18 | 1.1 | 0.09 | 18 | 3.3 | 0.24 | 18 | 1.3 | 0.12 |
| Swell period | 1 | 18 | 7.6 | 0.85 | 14 | 8.1 | 0.59 | 10 | 6.1 | 0.99 |
| | 2 | 18 | 7.4 | 0.85 | 16 | 8.6 | 1.33 | 7 | 6.1 | 1.48 |
| | 3 | 18 | 7.4 | 1.79 | 16 | 8.6 | 0.92 | 12 | 6.4 | 1.36 |
| Swell height | 1 | 18 | 2.0 | 0.22 | 14 | 3.0 | 0.36 | 11 | 1.2 | 0.16 |
| | 2 | 18 | 2.0 | 0.19 | 16 | 3.0 | 0.53 | 8 | 1.1 | 0.17 |
| | 3 | 18 | 1.9 | 0.07 | 16 | 3.1 | 0.45 | 13 | 1.1 | 0.13 |

Table 2. The average of each observational data classified into the ship's side
Left: The number of data
Right: The average (period: sec, height: m)
The parentheses show the windward side of wind-waves and the coming side of swells.
POR: Port
STA: Starboard

| | | A | | | | B | | | | C | | | |
|---|---|---|---|---|---|---|---|---|---|---|---|---|---|
| | | POR | | STA | | POR | | STA | | POR | | STA | |
| Wind-wave period | 1 | 7 | 3.6 | 10 | 3.8 | 8 | 6.1 | 9 | 6.2 | 7 | 3.6 | 10 | 3.7 |
| | 2 | 7 | 3.4 | 10 | 3.4 | 8 | 5.9 | 9 | 6.3 | 8 | 3.8 | 9 | 3.4 |
| | 3 | (8 | 3.4) | 9 | 3.4 | 7 | 5.7 | (10 | 6.6) | 8 | 3.8 | (9 | 3.4) |
| Wind-wave height | 1 | 7 | 1.1 | 10 | 1.2 | 8 | 3.3 | 9 | 3.7 | 7 | 1.2 | 10 | 1.7 |
| | 2 | 7 | 0.9 | 10 | 1.0 | 8 | 3.0 | 9 | 3.1 | 8 | 1.1 | 9 | 1.2 |
| | 3 | (8 | 1.1) | 9 | 1.0 | 7 | 3.2 | (10 | 3.4) | 8 | 1.3 | (9 | 1.3) |
| Swell period | 1 | (7 | 7.1) | 10 | 7.6 | (7 | 8.4) | 6 | 8.0 | (4 | 6.5) | 6 | 5.8 |
| | 2 | 7 | 7.6 | (10 | 7.5) | 6 | 8.5 | (9 | 8.8) | 4 | 6.3 | (3 | 6.0) |
| | 3 | (8 | 7.8) | 9 | 7.3 | 6 | 8.2 | (9 | 9.1) | 6 | 6.0 | (6 | 6.8) |
| Swell height | 1 | (7 | 2.0) | 10 | 2.0 | (7 | 3.2) | 6 | 3.0 | (4 | 1.1) | 7 | 1.2 |
| | 2 | 7 | 1.9 | (10 | 2.1) | 6 | 2.8 | (9 | 3.2) | 4 | 1.0 | (4 | 1.1) |
| | 3 | (8 | 1.9) | 9 | 1.9 | 6 | 3.2 | (9 | 3.2) | 6 | 1.1 | (7 | 1.1) |

The difference of the visual observational data reflecting the difference of sailing state relating to wind-wave direction was investigated. The sailing state was classified as head wave-, lee wave- and stopping conditions.

In the case of wind-wave height, there are clear characteristics of having a tendency that the data at stopping are larger than at lee waves and the data at head waves are almost predominant. The wave height at head waves is 5–10% larger and at lee waves it is 10–20% smaller than at stopping.

* At the observations B and C, there are no such data.

Moreover, in the variance of the wave period and height at head waves, there are a few characteristics that the scatter in the period is smaller and that of the height is larger than at the cases of lee waves or stopping.

In the case of swelles, as seen in Fig. 4, coming or going directions of swell as to the ships' position are not evident, therefore, these characteristics are not so clear in an average and a variance.

**4. The characteristics of the visual observational data reflecting the difference of the ship's observational side** (waves coming side or leaving side)

Table 2 shows the average* of the period and height of wind-waves and swells which were obtained from the nine observations. Observers who were stationed port side only observe noticeable wind-waves and swells at that side, and *vice versa*.

On wind-waves, it was expected that the data of both sides will be equal in the period and height at head waves and lee waves and the data of windward side will be larger than of leeward side at stopping, but it is not so clear in Table 2.

About the swells, they have a tendency that the period and height at a leaving side are within 10% smaller than at a coming side.

**5. The characteristics of the visual observational data reflecting the difference of the observational position height from the sea level**

Table 3 shows the average* of the period and height of wind-waves and swells

| | | A | | | | | | | | B | | | | | | | | C | | | | | | | |
|---|---|---|---|---|---|---|---|---|---|---|---|---|---|---|---|---|---|---|---|---|---|---|---|---|---|
| | | COM | | NAV | | F'C | | UPP | | COM | | NAV | | F'C | | UPP | | COM | | NAV | | F'C | | UPP | |
| Wind-wave period | 1 | 4 | 3.3 | 4 | 3.8 | 6 | 4.0 | 3 | 3.7 | 3 | 6.3 | 4 | 6.3 | 6 | 6.5 | 4 | 5.5 | 4 | 4.0 | 4 | 3.3 | 5 | 3.4 | 4 | 4.0 |
| | 2 | 4 | 4.0 | 3 | 3.7 | 6 | 3.2 | 4 | 3.0 | 4 | 6.8 | 4 | 4.8 | 5 | 6.2 | 4 | 6.8 | 4 | 3.5 | 4 | 3.8 | 6 | 3.7 | 3 | 3.3 |
| | 3 | 4 | 3.8 | 4 | 2.8 | 5 | 3.6 | 4 | 3.5 | 3 | 6.3 | 4 | 6.8 | 6 | 6.2 | 4 | 5.8 | 4 | 4.3 | 3 | 3.7 | 6 | 3.0 | 4 | 3.8 |
| Wind-wave height | 1 | 4 | 1.0 | 4 | 1.1 | 6 | 1.3 | 3 | 1.2 | 3 | 3.5 | 4 | 3.3 | 6 | 3.5 | 4 | 3.8 | 4 | 1.8 | 4 | 1.4 | 5 | 1.6 | 4 | 1.1 |
| | 2 | 4 | 1.0 | 3 | 1.0 | 6 | 0.8 | 4 | 1.0 | 4 | 3.1 | 4 | 2.9 | 5 | 3.0 | 4 | 3.1 | 4 | 1.1 | 4 | 1.0 | 6 | 1.3 | 3 | 1.0 |
| | 3 | 4 | 1.1 | 4 | 1.0 | 5 | 1.2 | 4 | 0.9 | 3 | 3.5 | 4 | 2.9 | 6 | 3.5 | 4 | 3.3 | 4 | 1.6 | 3 | 1.3 | 6 | 1.3 | 4 | 1.0 |
| Swell period | 1 | 4 | 7.3 | 4 | 7.0 | 6 | 7.7 | 3 | 7.7 | 3 | 8.7 | 3 | 7.7 | 5 | 8.0 | 2 | 9.0 | 4 | 6.5 | 1 | 5.0 | 4 | 6.3 | 1 | 5.0 |
| | 2 | 4 | 7.8 | 3 | 8.0 | 6 | 7.3 | 4 | 7.3 | 3 | 8.3 | 4 | 9.0 | 5 | 8.6 | 3 | 8.7 | 4 | 6.3 | 1 | 4.0 | 2 | 7.0 | 0 | - |
| | 3 | 4 | 6.0 | 4 | 7.8 | 5 | 8.0 | 4 | 8.3 | 3 | 8.3 | 3 | 8.7 | 5 | 8.6 | 4 | 9.3 | 0 | - | 2 | 5.5 | 6 | 6.3 | 4 | 7.0 |
| Swell height | 1 | 4 | 1.6 | 4 | 2.0 | 6 | 2.3 | 3 | 2.0 | 3 | 2.7 | 3 | 2.8 | 5 | 3.3 | 2 | 3.8 | 4 | 1.3 | 2 | 1.0 | 4 | 1.1 | 1 | 1.5 |
| | 2 | 4 | 2.0 | 3 | 2.2 | 6 | 1.8 | 4 | 2.1 | 3 | 3.0 | 4 | 3.8 | 5 | 2.5 | 3 | 3.2 | 4 | 1.1 | 1 | 0.5 | 3 | 1.2 | 0 | - |
| | 3 | 4 | 1.9 | 4 | 1.9 | 5 | 1.9 | 4 | 2.0 | 3 | 2.7 | 3 | 2.8 | 5 | 3.3 | 4 | 3.8 | 1 | 0.5 | 2 | 1.0 | 6 | 1.3 | 4 | 1.1 |

Table 3. The average of each observational data classified into the deck
Left: The number of data
Right: The average (period: sec, height: m)
COM: Compass BR. Deck
NAV: Navigation BR. Deck
F'C: F'CLE Deck
UPP: Upper Deck

* The data of the seaman at the navigation bridge were excluded.

which were obtained from nine observations and are classified into four height categories in terms of deck level for catching the characteristics which reflected the difference of the observational position height from the sea level, but it should be noted that the number of data used for calculating the average is rather small.

It was generally expected that the height of wind-waves and of swells may become higher as the observational position becomes lower, but such effect is not so evident in Table 2.

As to the wind-wave height only, there is a slight tendency that the data at Navigation Bridge Deck are smaller than at the next higher and lower decks.

## 6. The characteristics of the data reflecting the difference of the visual wave observational experience of observers

Table 4 shows the average and variance of the period and height of wind-waves

| | | A | | | | B | | | | C | | | |
|---|---|---|---|---|---|---|---|---|---|---|---|---|---|
| | | SKI | | UNS | | SKI | | UNS | | SKI | | UNS | |
| Wind-wave period | 1 | 9 3.4 | 0.78 | 9 3.9 | 0.61 | 9 6.3 | 0.50 | 9 6.2 | 1.19 | 9 3.9 | 0.61 | 9 3.4 | 0.28 |
| | 2 | 9 3.2 | 0.94 | 9 3.6 | 0.53 | 9 6.1 | 0.61 | 9 6.2 | 1.69 | 9 3.6 | 0.53 | 9 3.7 | 0.50 |
| | 3 | 9 3.1 | 0.86 | 9 3.7 | 0.50 | 9 6.1 | 0.36 | 9 6.4 | 1.78 | 9 3.6 | 0.53 | 9 3.7 | 0.50 |
| Wind-wave height | 1 | 9 1.2 | 0.19 | 9 1.2 | 0.06 | 9 3.7 | 0.25 | 9 3.3 | 0.51 | 9 1.5 | 0.06 | 9 1.4 | 0.30 |
| | 2 | 9 0.9 | 0.09 | 9 0.9 | 0.09 | 9 3.3 | 0.06 | 9 2.7 | 0.13 | 9 1.2 | 0.07 | 9 1.1 | 0.15 |
| | 3 | 9 1.2 | 0.06 | 9 0.9 | 0.09 | 9 3.4 | 0.11 | 9 3.2 | 0.38 | 9 1.3 | 0.06 | 9 1.2 | 0.19 |
| Swell period | 1 | 9 7.3 | 0.50 | 9 7.8 | 1.19 | 7 8.4 | 0.62 | 7 7.9 | 0.48 | 5 6.0 | 0.50 | 5 6.2 | 1.70 |
| | 2 | 9 7.6 | 1.03 | 9 7.3 | 0.75 | 8 8.9 | 1.27 | 8 8.3 | 1.36 | 2 6.5 | 0.50 | 5 6.0 | 2.00 |
| | 3 | 9 7.7 | 0.50 | 9 7.2 | 3.19 | 8 8.5 | 0.57 | 8 8.8 | 1.36 | 6 6.3 | 1.07 | 6 6.5 | 1.90 |
| Swell height | 1 | 9 1.9 | 0.34 | 9 2.1 | 0.11 | 7 3.3 | 0.32 | 7 2.8 | 0.32 | 5 1.0 | 0.13 | 6 1.3 | 0.17 |
| | 2 | 9 2.1 | 0.15 | 9 1.9 | 0.24 | 8 3.3 | 0.36 | 8 2.8 | 0.64 | 3 1.0 | 0.25 | 5 1.1 | 0.18 |
| | 3 | 9 1.9 | 0.09 | 9 1.9 | 0.05 | 8 3.3 | 0.64 | 8 3.0 | 0.29 | 7 1.1 | 0.14 | 6 1.1 | 0.14 |

Table 4. The average and variance of each observational data classified into the visual wave observational experience of observers.
Left: The number of data
Center: The average (period: sec, height: m)
Right: The variance
SKI: Skilled group
UNS: Unskilled group

and swells which were obtained from the nine observations by the two groups which were separated from the difference of the visual wave observational experience.

About the wind-wave height in this table, the data of unskilled group are 5–20% smaller than those of the skilled group. This fact is unrelated to the state of the sea and sailing, and the fact that the data of unskilled group being smaller by 5–20% is also recognized in the swell height in stormy weather as shown in observation B. The evident characteristics are found in the variance of the wind-wave height too, that is

to say, the scatter in the unskilled group's data is fairly larger than those of the skilled group's data unrelated to the state of the sea and sailing, and such large scattering in unskilled group is also recognized in the wind-wave period in stormy weather as shown in observation B.

### 7. The swell direction

The swell direction is one of the factors of visual wave observational data which are put to use for Ocean Wave Chart. However, directions of swell can be, to some extent, obtainable from the previous wave charts. Therefore, we put less importance for the swell direction data. As to swell direction, only apparent features are the following two.

As seen in Fig. 4, the scatter in the data is large* and there is no data for 90° either to the right or left.**

**Acknowledgments**

The author wishes to express his gratitude to the crew of the Keifu-maru who cooperated in getting these precious data. Special thanks are also bestowed upon the observers who fought stormy weather and mountainous waves to obtain these valuable data.

## 観測船「啓風丸」における目視波浪観測について

木 村 隆 昭
(気象庁海洋気象部)

気象庁海洋気象部により作成され毎日 FAX 放送されている外洋波浪実況図は，観測船や一般船舶における目視波浪観測データを基に作図されている。

これらのデータには，天気図上で見てほぼ同一海面状態と推定される海域内からの通報にもかかわらず，その値が大きく異なる例がしばしば見うけられる。その原因としては，向い波や追い波などの船の航走状態の違い，風上舷や風下舷および海面上の高さなどの船上における観測位置の違い，また観測者の熟練度の違いなどが考えられる。

そこで1974年4月に伊豆大島近海で啓風丸により実施された目視波浪観測の資料を基にこれらの関

* The scattering width is ranging from 100° to 200°.

** The bow direction being taken as 0°, and the number of data for 80° (port and starboard) is six, for 90°, zero, for 100°, nine.

係を調査したところ，次のような結果を得た。

①周期，波高，波向のすべての観測要素にわたり，観測値のばらつきが予想外に大きい。

②停船時にくらべ向い波時には5～10%大きく，また追い波時には10～20%小さく**風浪の波高**を観測する傾向がある。

③海面状態，航走状態のいかんにかかわらず，目視観測経験度の浅い観測者は経験度の深い観測者よりも5～20%小さく**風浪の波高**を観測する傾向がある。

④風浪が卓越してうねりがわかりにくい海面状態においては，目視観測経験度の浅い観測者は経験度の深い観測者よりも5～20%小さく**うねりの波高**を観測する傾向がある。

気象庁

# 欧文海洋報告

第 28 巻

# THE OCEANOGRAPHICAL MAGAZINE

Vol. 28

*Published by the Japan Meteorological Agency*

March, 1977

# CONTENTS

ISOZAKI, I. and E. KITAHARA: Tides in the Bays of Ariake and Yatsushiro.. 1
AKAGAWA, M.: Characteristics of Oceanographic Conditions in the Okhotsk Sea and Meteorological Conditions over the Far East in November ..... 33
KIMURA, T.: Visual Wave Observations on Board the R/V Keifu-maru..... 47